Structure and evolution of the eastern Gulf of Aden conjugate margins from seismic reflection data.

Elia d'Acremont, Sylvie Leroy, Marie-Odile Beslier, Nicolas Bellahsen, Marc Fournier, Cécile Robin, Marcia Maia, Pascal Gente

Geophys. J. Int. (2005) **160,** 869–890 doi: 10.1111/j.1365-246X.2005.02524.x

Structure and evolution of the eastern Gulf of Aden conjugate margins from seismic reflection data

Elia d'Acremont,[1] Sylvie Leroy,[1] Marie-Odile Beslier,[2] Nicolas Bellahsen,[3] Marc Fournier,[1] Cécile Robin,[4] Marcia Maia[5] and Pascal Gente[5]

[1] *CNRS-UMR* 7072, *Laboratoire de Tectonique, Université P. et M. Curie, Case* 129, 4 *place Jussieu,* 75252 *Paris Cedex* 05, *France. E-mail: dacremont@obs-vlfr.fr*
[2] *CNRS-UMR* 6526, *Géosciences Azur, Observatoire Océanologique,* BP48, 06235 *Villefranche sur mer Cedex*
[3] *Division Géologie–Géochimie, Institut Français du Pétrole,* 1-4 *avenue de Bois Préau,* 92852 *Rueil Malmaison, France*
[4] *CNRS-UMR* 6118, *Géosciences Rennes, Université de Rennes* 1, *Bât.* 15, *Campus de Beaulieu, France*
[5] *CNRS-UMR* 6538, *Domaines Océaniques, IUEM, Place Nicolas Copernic,* 29280 *Plouzané, France*

Accepted 2004 November 8. Received 2004 November 2; in original form 2004 June 18

SUMMARY

The Gulf of Aden is a young and narrow oceanic basin formed in Oligo-Miocene time between the rifted margins of the Arabian and Somalian plates. Its mean orientation, N75°E, strikes obliquely (50°) to the N25°E opening direction. The western conjugate margins are masked by Oligo-Miocene lavas from the Afar Plume. This paper concerns the eastern margins, where the 19–35 Ma breakup structures are well exposed onshore and within the sediment-starved marine shelf. Those passive margins, about 200 km distant, are non-volcanic. Offshore, during the Encens–Sheba cruise we gathered swath bathymetry, single-channel seismic reflection, gravity and magnetism data, in order to compare the structure of the two conjugate margins and to reconstruct the evolution of the thinned continental crust from rifting to the onset of oceanic spreading. Between the Alula-Fartak and Socotra major fracture zones, two accommodation zones trending N25°E separate the margins into three N110°E-trending segments. The margins are asymmetric: offshore, the northern margin is narrower and steeper than the southern one. Including the onshore domain, the southern rifted margin is about twice the breadth of the northern one. We relate this asymmetry to inherited Jurassic/Cretaceous rifts. The rifting obliquity also influenced the syn-rift structural pattern responsible for the normal faults trending from N70°E to N110°E. The N110°E fault pattern could be explained by the decrease of the influence of rift obliquity towards the central rift, and/or by structural inheritance. The transition between the thinned continental crust and the oceanic crust is characterized by a 40 km wide zone. Our data suggest that its basement is made up of thinned continental crust along the southern margin and of thinned continental crust or exhumed mantle, more or less intruded by magmatic rocks, along the northern margin.

Key words: continental margins, Gulf of Aden, ocean–continent transition, plate divergence, rifted margin, seafloor spreading.

1 INTRODUCTION

Non-volcanic passive margins are usually described in three different domains (e.g. Boillot *et al.* 1988), namely (1) the continental domain, where the basement is structured in a series of basins and basement rises, (2) the true oceanic domain, where the bathymetry is relatively smooth, and (3) in between them, a transitional domain referred to as the oceanic–continental transition (OCT), where the basement is partly composed of exhumed mantle. Recent geophysical explorations (South Armorican, Newfoundland and southwest Australian margins, South Labrador, Ligurian and Tyrrhenian seas: e.g. Chian *et al.* 1995; Mauffret *et al.* 1999; Thinon *et al.* 2001; Rollet *et al.* 2002; Beslier *et al.* 2004; Hopper *et al.* 2004) suggest that the OCT is characterized by non- or poorly volcanic continental breakup zones.

Models for non-volcanic margins differ in the role played by crustal- or lithospheric-scale fault zones in accommodating strain, as well as in the degree of asymmetry between the conjugate margins—i.e. pure shear (McKenzie 1978), simple shear (Wernicke 1985) or intermediate models (Lister *et al.* 1986). The degree of symmetry between the margins may also depend on the structural inheritance prior to the rifting. Indeed, pre-existing faults could generate deep and shallow asymmetrical structures on the margins. The structural pattern and its evolution can be also guided by the degree of

obliquity between the rift and the opening trend (Tron & Brun 1991; McClay & White 1995; Bonini *et al.* 1997).

Extensive work has been devoted to studying passive margins all over the world. Yet only a small part of this work has been dedicated to conjugate passive margins. This is mainly because the further the margins drift apart, the less accurate is the match between the conjugate margins and the thicker is the overlying post-rift sedimentary sequence. This makes it more difficult to investigate syn-rift features and to link onshore and offshore structures. However, the joint analysis of conjugate margins greatly improves our understanding of rifting processes and of the rifting/spreading transition. This includes the degree of symmetry of the rifted zones, the geometry and the inception sequence of fault systems from the external to the internal domains, the characterization of the OCT, and the spatiotemporal evolution of the segmentation.

In this paper we study the most recent conjugate passive margins worldwide, in the Gulf of Aden. This is an appropriate site for comparing conjugate margins and for studying lithospheric breakup from continental rifting to seafloor spreading, for the following reasons:

(1) This young and narrow basin allows conjugate margins to be closely correlated.

(2) Both margins are well preserved beneath a thin post-rift sedimentary cover.

(3) The rifting is oblique, as predicted by the regional plate kinematics (Jestin *et al.* 1994).

(4) There are pre-existing Mesozoic basins in the area of the future Gulf of Aden. Moreover, its northern and southern offshore margins both crop out on land (Fig. 1) and the study area is located in the eastern part of the Gulf, away from the Afar hotspot, where the margins are supposed to be non- or only weakly volcanic.

The oceanic part of the Gulf of Aden has been extensively surveyed (Laughton & Tramontini 1969; Cochran 1981; Tamsett & Searle 1988; Sahota 1990; Schilling *et al.* 1992; Manighetti *et al.* 1997; Audin *et al.* 2001). To date, most offshore studies have been conducted in its western part, where volcanic margins have been identified (Tard *et al.* 1991), whilst the eastern part has only been studied on land (Roger *et al.* 1989; Bellahsen *et al.* in press, and references therein).

Our purpose is to test current models of continental breakup using new data from the offshore sector of the eastern Gulf of Aden. This study is based upon the geophysical data gathered during the Encens–Sheba cruise between the Alula-Fartak and the Socotra fracture zones (June 2000; Leroy *et al.* 2000, 2004). The interpretation of the magnetic and gravity data of the Encens–Sheba cruise will be presented in a complementary paper (d'Acremont *et al.* submitted).

2 GEODYNAMICAL AND GEOLOGICAL SETTINGS

2.1 The Gulf of Aden

Through the Arabia–Somalia Plate, successive Jurassic and Cretaceous rifting episodes have created major basins (from west to east the Balhaf, Masilah, Jeza, Qamar, Phoenix and Rukh basins; see inset to Fig. 1) (Bott *et al.* 1992; Beydoun *et al.* 1996; Bosence 1997). These basins have a predominant east–west to northwest–southeast orientation. In Oligocene times the Afro Arabian Plate began to separate due to the creation of two divergent basins, which both evolved in narrow oceanic basins: the Red Sea to the west, between Arabia and Africa (Nubia) and the Gulf of Aden to the south, between Arabia and Somalia. Still in a rifting stage, the East African rift forms the third branch of the Afar ridge–ridge–ridge type (RRR) triple junction (Wolfenden *et al.* 2004). This later Oligo-Miocene stretching episode of the Arabia–Somalia Plate reactivated inherited structures of these Mesozoic basins (see inset to Fig. 1) (Ellis *et al.* 1996; Granath 2001; Bellahsen 2002).

The Gulf of Aden extends from the Owen fracture zone (58°E) to the east to the Afar to the west (43°E), where the Aden Ridge enters through the Gulf of Tadjoura (Fig. 1). The spreading rate increases from west (1.6 cm yr^{-1} along N37°E) to east (2.34 cm yr^{-1} along N26°E). At the longitude of the study area (14.4°N and 53°E), the spreading rate is 2.2 cm yr^{-1} along a N25°E direction (Jestin *et al.* 1994; Fournier *et al.* 2001). Therefore, the mean extension direction is oblique to the mean trend of the Gulf of Aden (N75°E).

Oceanic spreading started in the eastern part of the Gulf at 17.6 Ma (A5d) (Sahota 1990; Leroy *et al.* 2004). Spreading probably started slightly later in the western part of the Gulf where the anomaly A5c was identified (Cochran 1981; Huchon & Khanbari 2003).

The early stage of the Gulf of Aden is contemporaneous with the youngest continental flood basalt province, related to the Afar hotspot (~30 Ma) (Schilling 1973; Courtillot 1980; Ebinger & Hayward 1996; Menzies *et al.* 1997); this caused the formation of volcanic margins in the western part of the Gulf. The Gulf of Aden is divided into three parts by two major discontinuities (Manighetti *et al.* 1997). The westernmost one is the Shukra-El Sheik discontinuity (Fig. 1). It may correspond to the limit of influence of the Afar hotspot and to a major change in the rheology of the lithosphere (Manighetti *et al.* 1998; Dauteuil *et al.* 2001; Hébert *et al.* 2001). The Alula-Fartak fracture zone separates the central part from the eastern one (Tamsett & Searle 1990). Our study area is located between the Alula-Fartak and the Socotra fracture zones. The horizontal offset of the Alula-Fartak transform fault is about 180 km, and transforms the Sheba Ridge to the Aden Ridge, in the vicinity of the southern margin.

2.2 Geological history of onshore margins

The results of earlier field studies allow us to summarize the structure and the tectono-sedimentary evolution of the eastern margins (Figs 2 and 3) (Roger *et al.* 1989; Fantozzi & Ali-Kassim 2002; Huchon & Khanbari 2003; Bellahsen *et al.* in press, and references therein).

2.2.1 Oman–Yemen northern margin

The northern rifted margin is exposed in the Dhofar area, southern Oman and in eastern Yemen (Fig. 2A). It is formed by a Cretaceous to Eocene platform cut by several basins of mean direction N100°E. The major basins are the Salalah Plain and the Ashawq Graben, both partly filled with syn-rift Oligo-Miocene sedimentary formations. These basins are composed of fault segments whose orientation ranges from N70°E to N110°E, and are bounded by southward-dipping normal faults (Lepvrier *et al.* 2002; Bellahsen *et al.* in press). In terms of pre-, syn- and post-rift deposits, the Tertiary sedimentary succession is formed respectively by the Hadhramaut, Dhofar and Fars groups (Fig. 2A) (Roger *et al.* 1989).

The pre-rift Hadhramaut Group is Palaeocene to Eocene in age. It is a wide monoclinal plateau unconformably overlying a Proterozoic basement. Prior to the Oligo-Miocene rifting, the Afro-Arabian platform underwent a major uplift which induced a

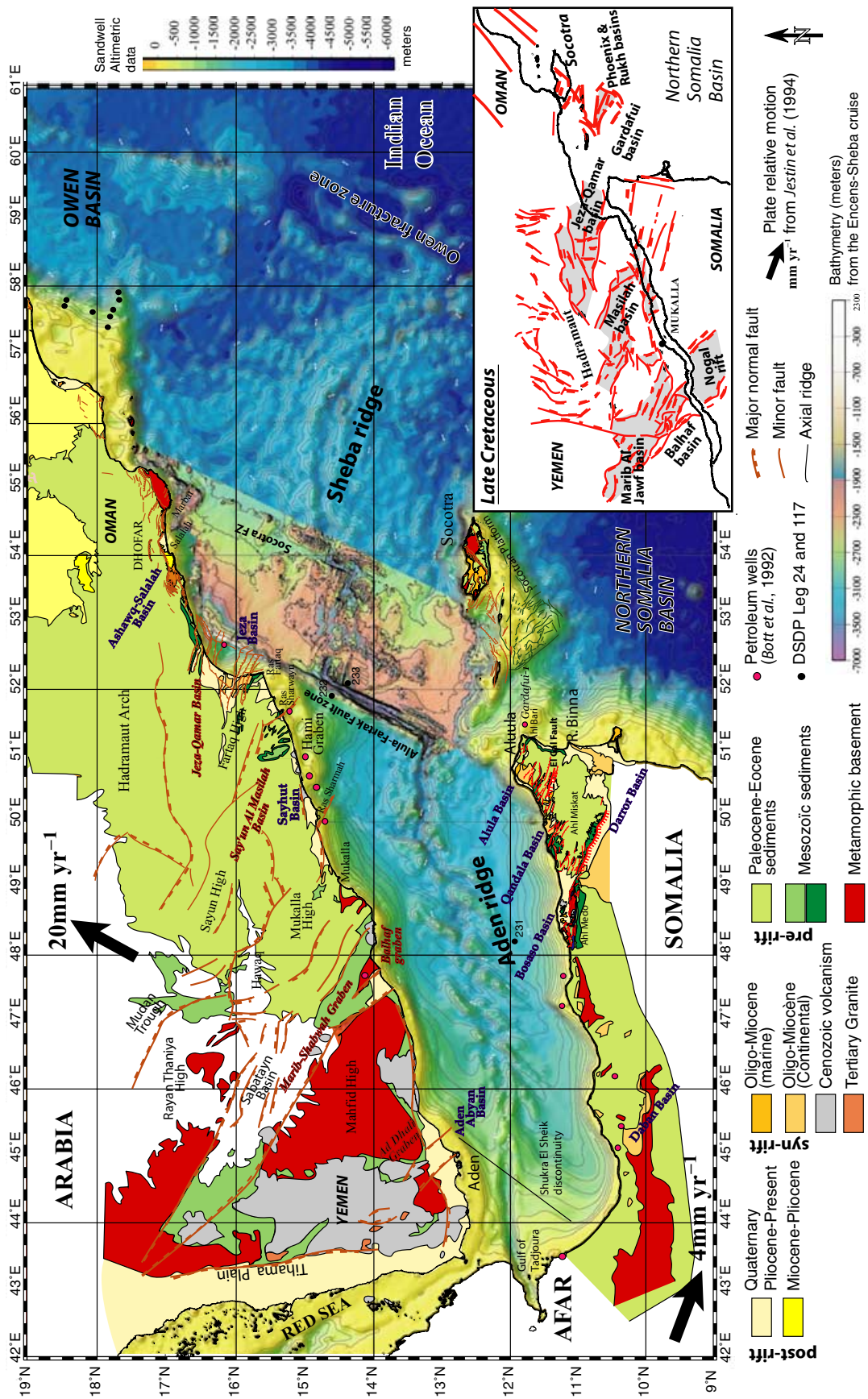

Figure 1. Bathymetry and topographic map of the Gulf of Aden from Sandwell & Smith (1997) and the Encens–Sheba cruise (swath bathymetry). Geological and structural map of the Gulf of Aden, onshore area (synthesis from Beydoun & Bichan 1969; Roger *et al.* 1989; Platel *et al.* 1992; Menzies *et al.* 1994; Fantozzi 1996; Birse *et al.* 1997; Brannan *et al.* 1997; Morrison *et al.* 1997; Samuel *et al.* 1997; Watchorn *et al.* 1998). Inset: sketch of the Mesozoic basins before the Oligo-Miocene Gulf of Aden opening (modified from Ellis *et al.* 1996).

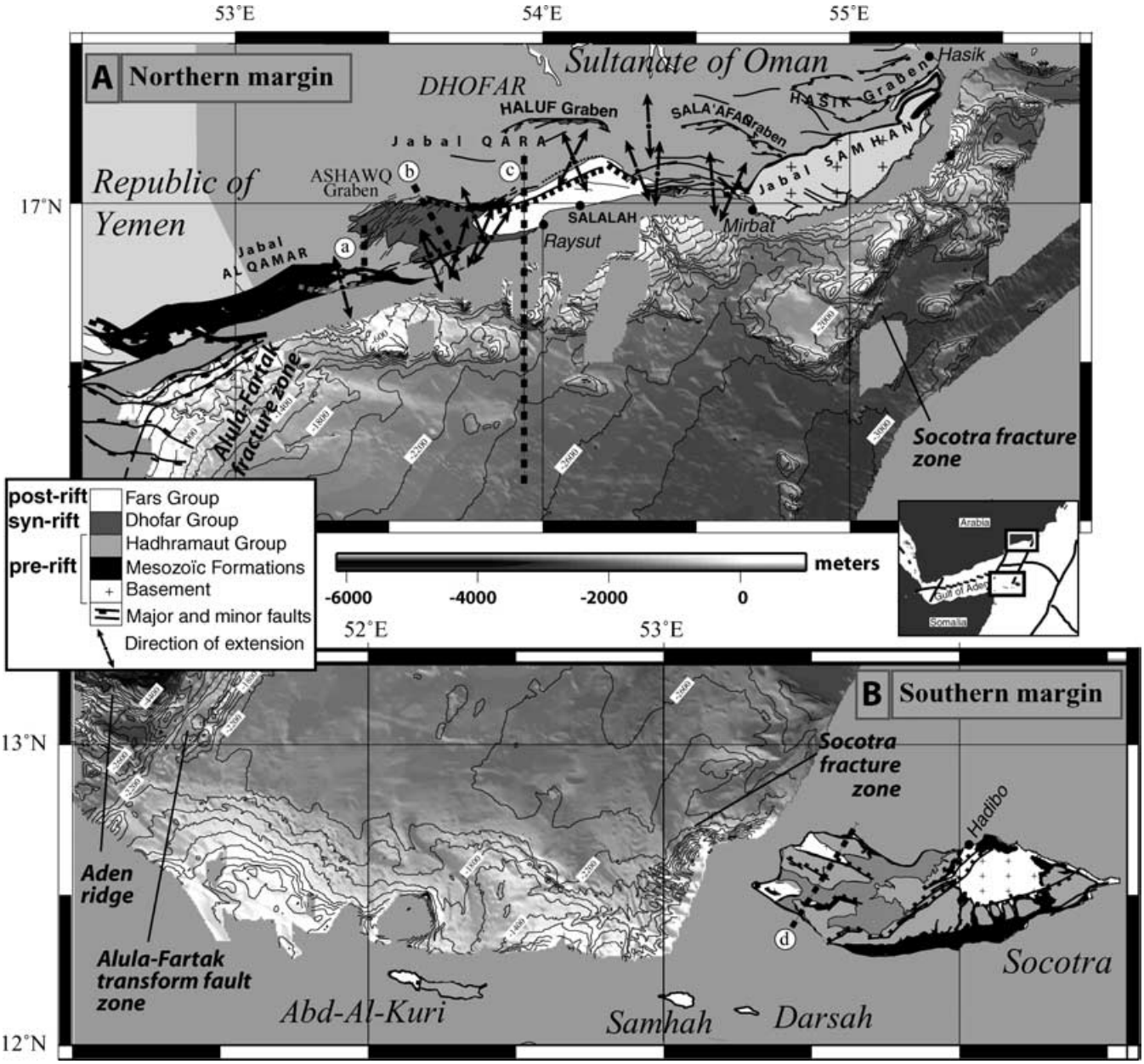

Figure 2. Structural sketch of the conjugate margins and swath bathymetric map of the onshore–offshore studied margins. (A) Northern margin, modified from Brannan *et al.* (1997), Lepvrier *et al.* (2002) and Bellahsen *et al.* (in press). Arrows show directions of extension inferred from fault slip data. (B) Southern margin, modified from Beydoun & Bichan (1969) and Birse *et al.* (1997).

non-deposition/erosion environment during the late Eocene (Platel & Roger 1989).

In Oman, the syn-rift sediments (Dhofar Group) range from 35 to 18 Myr in age (Roger *et al.* 1989). Their maximum thickness is about 1400 m (Fig. 3). From base to top, the sedimentary sequence show a deepening of the platform. In Yemen, the syn-rift sediments (Shihr Group) crop out within Mesozoic basins like the Qamar Basin (Bott *et al.* 1992; Huchon & Khanbari 2003). Two syn-rift extensional phases were recorded along the northern margin of the Gulf of Aden in Yemen (Huchon & Khanbari 2003) and in Oman (Fig. 2A) (Lepvrier *et al.* 2002). According to these authors, the N20°E extension pre-dates the N160°E one, and Huchon & Khanbari (2003) propose a two-stage model of opening of the Gulf of Aden which involves the propagation of a N75°E-trending lithospheric crack.

The onset of seafloor spreading in middle to upper Miocene time is correlated with the oldest post-rift sediments (Fars Group). Through the onshore domain, post-rift sedimentation occurred in narrow basins close to the coastline. During spreading, the sedimentary sequences are characterized by a deposit comparable with the present environment (Roger *et al.* 1992). This suggests that the Dhofar area acquired its present morphostructure in the Miocene, i.e. at the beginning of post-rift deposition.

2.2.2 Somalia–Socotra southern margin

East of Somalia, successive syn- and post-rift sequences crop out in basins, plateaus and mountains, limited by conjugate listric normal faults trending WNW–ESE (Figs 1 and 2B). The southern boundary of the margin is the southwest-dipping Darror Fault which crosses

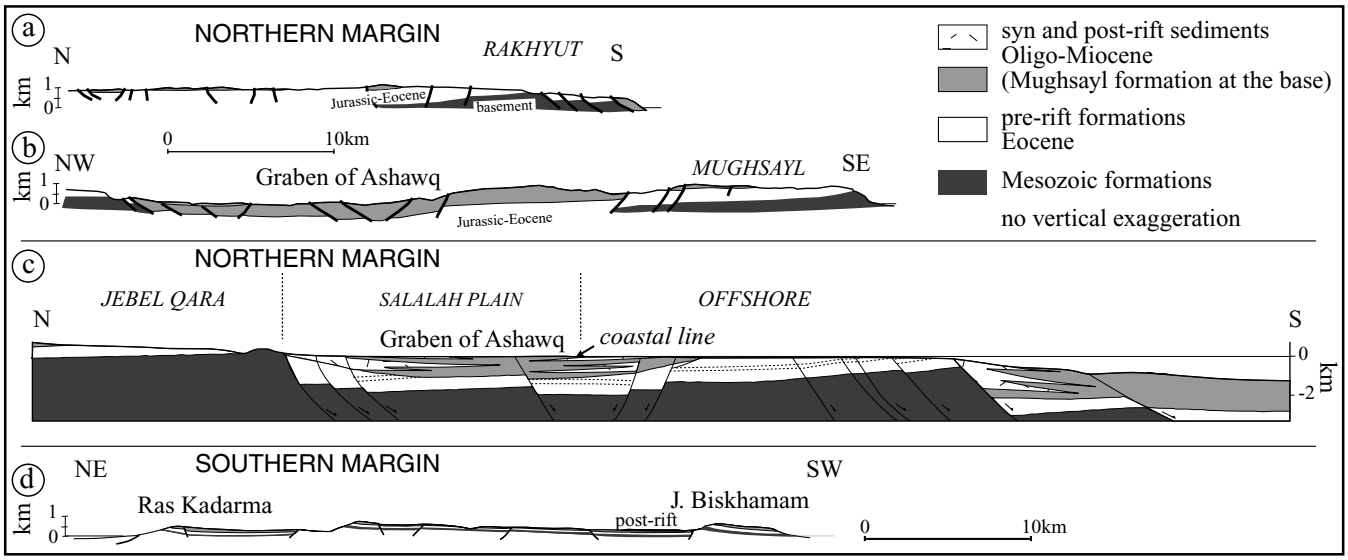

Figure 3. Cross-sections of the Dhofar area with no vertical exaggeration: a, b modified from Lepvrier *et al.* (2002); c from an unpublished line; and d through Socotra Island (modified from Beydoun & Bichan 1969; Birse *et al.* 1997; Samuel *et al.* 1997). See Fig. 2 for location.

the Horn of Africa from coast to coast (Fig. 1). It bounds the Darror Basin where Oligo-Miocene syn-rift formations are identified in eastern Somalia.

The pre-, syn- and post-rift sequences in northeastern Somalia are known from surveys conducted by Fantozzi & Ali-Kassim (2002). Similarly to the northern margin, the onshore southern margin exhibits a pre-rift series unconformably covered by transgressive syn-rift series. Syn-rift sediments, Oligo-Miocene in age, crop out in WNW–ESE-trending basins along the Gulf of Aden coasts. These formations consist of continental deposits, followed by platform and finally neritic deposits. The oldest syn-rift sediments, Rupelian in age, date the onset of rifting in the lower Oligocene (Fantozzi & Sgavetti 1998). The youngest deposits are 27 to 22 Myr old (Ali-Kassim 1993).

Further east, the Socotra Platform forms a bathymetric high which is the easternmost end of the Horn of Africa. Socotra Island is affected by N45°E-trending normal faults, which separate the island into two parts (Fig. 2B). The eastern part of the island is mainly composed of crystalline Cambrian basement unconformably covered by pre-rift calcareous sediments (Beydoun & Bichan 1969). In the western part of the island, tilted blocks are bounded by N140°E- and N110°E-trending normal faults, which cut through Cretaceous to Miocene sediments (Fig. 3d). Birse *et al.* (1997) proposed that three extensional phases, related to Arabian, African and Indian breakups, are recorded on the Socotra Platform. The N45°E direction is related to the breakup of the Indian and Somalian plates and to the opening of the northern Somalia Basin in the Jurassic. The Late Cretaceous reconstruction map (Fig. 1, inset) shows that they may have been reactivated as transcurrent faults during the opening of the Gulf of Aden. The N140°E trend, mainly observed on the platform (Phoenix Basin), is associated with the rifting of the Neo-Tethys between the Afro-Arabian and Laurasian plates. The N110°E-trending faults are related to the last Oligo-Miocene rifting.

3 DATA COLLECTION

During the Encens–Sheba cruise of the R/V *Marion Dufresne* (2000 July), three-channel seismic reflection, bathymetric, magnetic and gravity data were collected on both margins and in the basin (Leroy *et al.* 2004). The seismic reflection data were acquired using a three-channel, 150 m long hydrophone streamer AMG 37/43. The source was formed of an array of two S80 water guns, with a volume of 1.3 l (80 in^3), each at a pressure of 140 bar. The firing rate was every 8 s from ES04 to ES09 profiles, and every 10.45 s from ES10 to ES100 (last) profiles in order to keep a maximum coverage of three. All profiles were processed using standard techniques, namely filters, three-fold stack and F–K migration. In addition, coherence-enhancing filters were applied in order to better image the reflectors. Note that in spite of a relatively weak penetration due to the characteristics of the acquisition system, the image quality is good enough to identify faults and sedimentary deposits in both continental and oceanic domains.

Following improvements, the Thomson Marconi Sonar TSM 5265 multibeam echo sounder of R/V *Marion Dufresne* provided remarkable data in terms of spatial resolution (about 50 m). Data were processed on board using the Caraïbes software developed by IFREMER to obtain 100 m space bathymetric grids (Leroy *et al.* 2000).

Our interpretation of the offshore data is supported by onshore field data. The offshore knowledge of the sedimentary series is based on a few petroleum (Bott *et al.* 1992) and DSDP drill holes (231 to 233 sites of Leg 24; Fisher *et al.* 1974), which are all located beside the study area (Fig. 1). The Encens–Sheba seismic profiles have been cross-correlated with some older profiles (single-channel seismic (SCS) from R/V *Shackleton* in 1979 Sahota, 1995 and unpublished MCS). In the Socotra Archipelago, data and interpretations from a reflection seismic database acquired in 1976 (provided by the OEPB) and by BGE& P in 1993 (Birse *et al.* 1997) are also incorporated into this study, as well as the seismic data for the Jeza Qamar Basin published by Brannan *et al.* (1997).

4 MORPHOSTRUCTURE OF THE OFFSHORE CONJUGATE MARGINS

4.1 Major morphostructural features

The multibeam bathymetric and the depth-to-basement maps (Figs 2 and 4) allow us to describe the main morphostructural

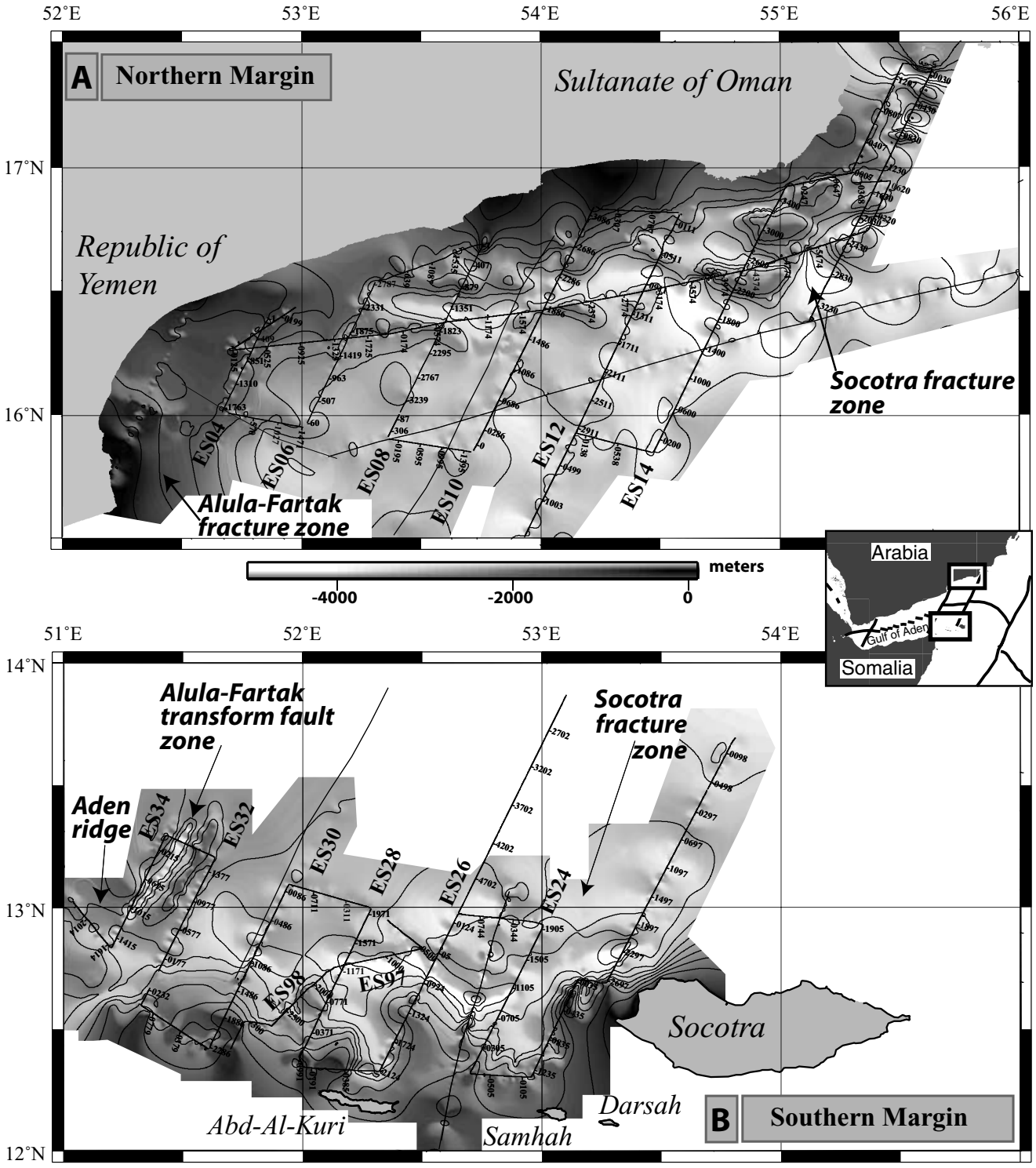

Figure 4. Depth of basement map. Depths to basement, in metres, are calculated from a mean velocity profile on single-channel and several multichannel seismic profiles. The contour interval is 500 m. Location of the profiles ES: Encens–Sheba seismic reflection profiles. Part (A) shows the north margin and (B) the south margin.

features of the two margins. Fig. 4 presents depth-to-basement maps of the conjugate margins compiled from the seismic reflection data. The top of the acoustic basement, usually marked by a strong reflector, is defined as the deepest continuous seismic horizon. It is determined by interpolating the isobaths from one profile to another. Depth conversion was made according to velocities from a few petroleum (Bott *et al.* 1992) and DSDP drill holes (sites 231 to 233 of Leg 24; Fisher *et al.* 1974) only available in the western part of the Gulf. *P*-wave velocities of 1.8, 2, 3 and 3.5 km s^{-1} were used in the post- and syn-rift sediments and in the acoustic basement respectively.

Fig. 2(a) shows the multibeam bathymetric map of the northern margin. Westward, the margin abuts against a steep northeast–southwest slope which marks the Alula-Fartak fracture zone.

Eastward, the N26°E Socotra fracture zone is a deep, elongated northeast–southwest basin whose western flank is steeper than the eastern one. The abyssal plain deepens eastward from 2 to 3 km. The continental slope, offshore of southern Yemen and Oman, is steep, narrow and is deeply cut by several canyons. Syn-rift features appear as WNW–ESE discontinuous elongate bathymetric highs and basins. On the depth-to-basement map (Fig. 4A), the margin is characterized by a series of alternate horsts and grabens trending N100°E to N110°E, i.e. oblique to the coastline, which are discontinuous and shifted toward the northeast. The top of the acoustic basement deepens eastwards from 1.5 to 4 km below sea level (bsl).

One peculiar feature of the southern region (Figs 1 and 2B) is the location, west of the Alula-Fartak transform fault, of the Aden spreading ridge, at the latitude of the southern margin (4500 m deep nodal basin situated at longitude 51°15E). The Alula-Fartak transform fault is characterized along the margin by a 3.6 km deep basin, trending N26°E, in which 1.2 km of sediments are accumulated (Fig. 4B). The eastern limit of this fault zone is a parallel and prominent (1.8 km bsl) linear horst, bounded by two transtensive normal faults (Fig. 4B). The southern part of the transform fault, which bounds the Aden Ridge, is much wider and includes an enlarged basin and an additional parallel ridge. Eastward, the Socotra fracture zone is well marked by the western steep slope of Socotra Island (12.5°N; 53°E), along which a northward shift of 50 km occurs. The abyssal plain deepens eastwards, with depths ranging from 2.2 to 2.6 km bsl. A coincident deepening of the acoustic basement from 0.5 to 4.8 km bsl is observed (Fig. 4B). Due to a thicker sedimentary cover that wraps and seals the margin structure, the continental slope is less abrupt and narrow than on the northern margin and the morphology is everywhere smoother. Southward, the continental platform locally emerges on the Socotra, Abd'al Kuri, Samhah and Darsah islands (Fig. 2B). Elsewhere, the very low mean water depth (∼30 m) prevented us from extending our survey southwards.

On the margin, the basement ridges and sedimentary basins have a mean N110°E direction (Fig. 4B). A large and deep basin (depth 4.5 km bsl) filled with a thick sedimentary sequence (2 km) is located at the foot of the margin (12.65°N, 52.75°E). Its curvilinear shape is due to variously oriented faults with strikes ranging from N40°E to N80°E, which are relatively well constrained with several seismic profiles crossing the basin (profiles ES28, ES26, ES24 and ES97–98; Fig. 4). From west to east, the basement highs are shifted twice toward the north (at 52.25°E and 53°E).

4.2 Identification of three domains on each margin

Three domains can be defined on each margin according to the seismic facies of the acoustic basement. From the continent toward the ocean, they are:

(1) The continental domain where the basement is structured in a series of basins and structural basement ridges that locally protrude through sedimentary cover.

(2) The transitional domain (OCT) where comparable tectonic features are buried under the sedimentary cover.

(3) The oceanic domain where the basement topography is relatively smooth.

4.2.1 Continental domain

Four unconformities are identified in the syn- and post-rift sequences on both margins (Fig. 5a).

In the basins, the syn-rift sedimentary sequence, unconformable on the acoustic basement, is generally made of deformed sediments which locally display a fan-shaped geometry. The basal series are essentially gravity-flow deposits without internal structure. The upper series are layered and display continuous seismic reflectors. Moreover, locally on the northern margin, the syn-rift sedimentary sequence displays two superimposed fan-shaped series with opposite

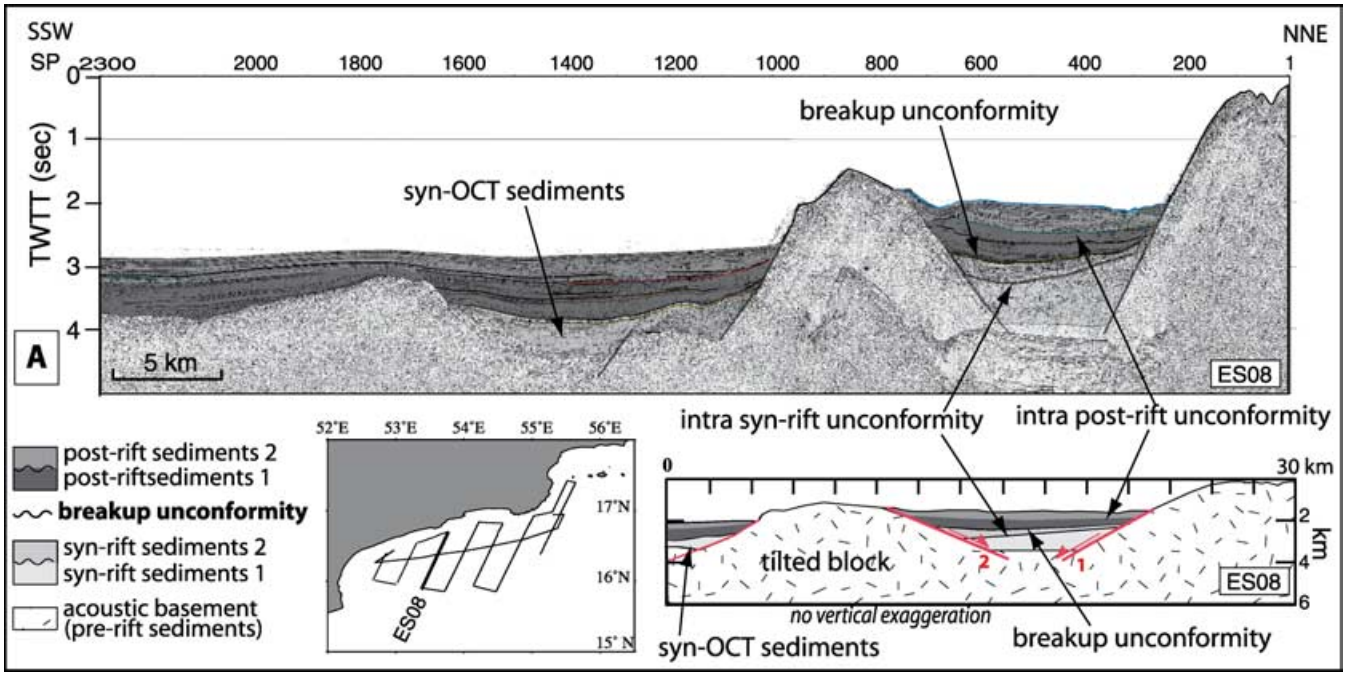

Figure 5. (A) Detail of a northern rifted basin (ES08 seismic profile) with the different sedimentary sequences identified on all profiles of the two margins. (B) ES10 profile of the central part of the north margin. Magnetic and free-air gravity anomalies with the OCT boundaries are reported. Migrated seismic line and its interpretation. (c) ES14 profile of the eastern part of the north margin. Migrated seismic line and its interpretation. See inset map in (A) for the location.

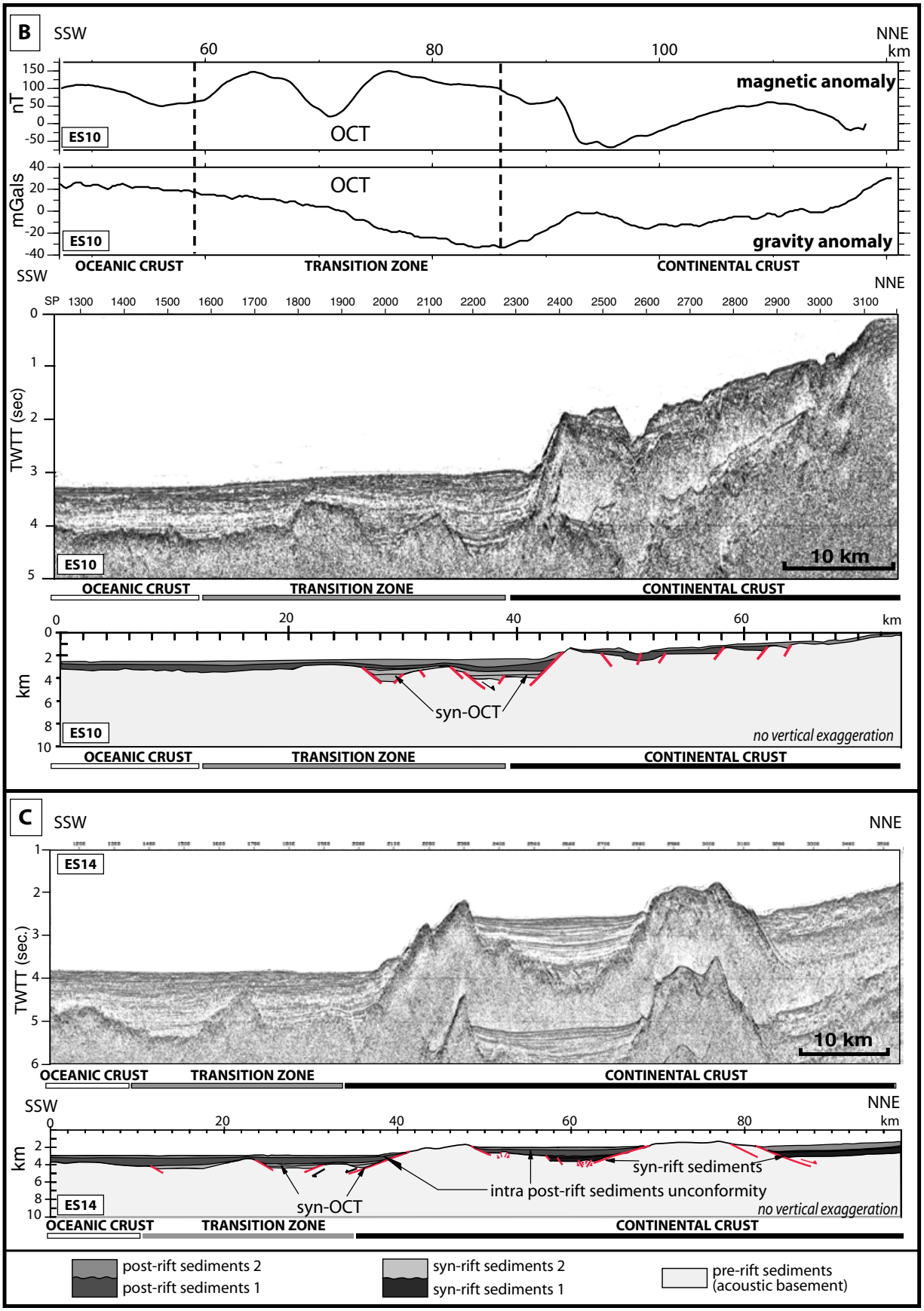

Figure 5. (*Continued*.)

vergence (syn-rift 2 overlying syn-rift 1; Fig. 5a): syn-rift 1 is associated with an oceanward-dipping fault and syn-rift 2 with a fault dipping toward the continent. An intra-syn-rift unconformity separates these opposite fan-shaped series. However, these fault kinematics may not be generalized to the whole rift. Sedimentary wedge superposition is observed in the suspended basin of the north margin and in the rifted basin of eastern Somalia (Fantozzi & Sgavetti 1998). Fan-like wedges exist along the northward-dipping faults, which mark the foot of the south margin continental slope.

The third major unconformity corresponds to the breakup unconformity between the syn-rift and the post-rift series. It is characterized by a toplap geometry of the syn-rift reflector's end and dates the end of the rifting episode.

The fourth unconformity is within the post-rift sequence. The lower post-rift unit 1 is eroded on the top. Its seismic sequence is characterized by a hummocky seismic facies interbedded with continuous high-amplitude horizontal reflectors. It shows that some tectonic activity still occurred after the end of the syn-rift episode. Post-rift unit 2 is characterized by slumping at the foot of the slope, and continuous reflectors toward the basin. Both post-rift series are present on the whole oceanic domain and on the offshore continental margins.

On the conjugate margins, the mean apparent dip of the normal faults is 30°. Such a low value may be due to seismic acquisition. As shown by Thomas *et al.* (1996), a series of steep parallel close faults imaged by high-resolution seismic data appears as a unique lower dipping fault on conventional seismic data. This pseudo-fault corresponds to the hyperbola envelope of the steeper faults.

Northern continental margin. The whole northern margin is composed of two large horsts and one or two suspended basins. It displays the previously described four-sequence stratigraphy (Figs 5b and c). The 6–12 km wide horsts are slightly tilted toward the continent (see ES14 on Fig. 5c). They delineate a 20 km wide suspended basin which appears asymmetric, bounded by one or a few northern faults and several smaller antithetic faults (ES14; Fig. 5c). The cumulative throw of the northern border faults is about 6 km (Fig. 5c, ES14).

The two syn-rift series are identified in the suspended basin (Fig. 5a, ES08). Indeed, the lower syn-rift (1) infill is related to southward-dipping faults and minor subsequent northward-dipping faults (maximum total throw equal to 5 km). In the upper syn-rift deposit (2), a slight fan along the north-dipping faults is observed. The last movement on these faults therefore occurred during the late stages of rifting. The total thickness of the syn-rift sequence is highly variable but it never exceeds 1200 m.

The syn-rift sedimentary sequences are not clearly imaged and are probably thinner in the suspended continental part of the ES10 profile. We note that in this central part of the margin, the continental slope is cut by deep canyons (ES10, Fig. 5b; SP 2500–2700), which cut the post-rift series in the prolongation of the wadis (Fig. 2). The horst is also broken by numerous southward-dipping faults. Although a poor penetration of the seismic waves cannot be completely excluded, the lack of syn-rift series in this part of the margin may rather be due to a non-depositional environment and/or to a later phase of erosion. This could be related to a local uplift or to a more diffuse deformation which prevented the development of deep grabens and of thick syn-rift deposits.

Southern continental margin. The seismic profiles crossing the southern margin in the survey area (Figs 6a and b) show one or two ∼20 km wide basement ridges, which delineate a suspended (>20 km wide) and deep (∼−4000 m) basin (ES28, Fig. 6b). The trend of these extensive structures is about N110°E. Most structural basement highs are buried under post-rift sediments. The north flank of the deeper high is intensely structured by a series of northward-dipping faults. The deeper ones delineate a narrow 4 km wide tilted block. Fan-shaped wedges of syn-rift deposits are developed along the northward-dipping faults (syn-rift 1, Figs 6a, b). The maximum apparent throw of the major normal faults is about 4 km. The suspended basin is asymmetric. It exhibits a maximum syn-rift sediment thickness in the north along the main southward-dipping fault and several antithetic faults. The bottom of the basin is dipping southward. The deep syn-rift sedimentary sequence is characterized by important slope deposit (SP 600, Fig. 6a). The maximum thickness of the total syn-rift formation reaches 750 m.

4.2.2 Transitional domain

The joint analysis of seismic reflection, free-air gravity and magnetic anomalies (Fig. 5b) reveals on each margin a narrow (20–30 km) transitional zone between the oceanic and the continental domains (OCT), characterized by peculiar features:

(1) The acoustic basement is clearly faulted and completely buried beneath the sediment cover. It displays a basin, which is generally asymmetric and bounded towards the continent by a major oceanward-dipping normal fault that marks the foot of the continental slope. Its oceanward flank is outlined on the northern margin and locally on the southern one (ES28; see Fig. 8), by one or two horsts.

(2) The occurrence of faulted sediments is contemporaneous with the deformation of the basement in the OCT. These sediments are observed only in the OCT basin. They do not exist on the adjacent oceanic crust. On the available seismic profiles, the correlation between these faulted sediments and the syn-rift sequences is generally difficult due to the protruding basement. We have thus to distinguish both of them by calling these OCT deposits syn-OCT sediments, probably related to the upper syn-rift sequence. These syn-OCT sediments are covered by post-rift 1 deposits as are the upper syn-rift series.

(3) A negative gradient of the free-air gravity anomaly from oceanic to continental domains is due to the edge effect generated by the juxtaposition of two types of crust.

(4) The magnetic data are generally quiet and flat, but locally display high-amplitude anomalies.

Northern margin OCT. As illustrated on the ES10 profile, the OCT of the northern margin, which is about 20 km wide, is characterized by a negative gradient of the free-air anomaly toward the continental crust, a magnetic quiet zone northward of the OCT, as well as by a faulted basin at the foot of the continental slope (Figs 5 and 7a–b). The sedimentary cover includes an unconformity between two distinct series: the deepest one, up to 900 m thick, is the syn-OCT previously described, and the upper one is a typical post-rift 1 sequence. The transitional basement is structured in basins and highs. The width of the basins along the margin depends on the number and geometry of basement highs. On the ES12 profile, one wider horst (about 15 km), displays an intense fracturing which delineates a small basin, and associated low-amplitude magnetic anomaly (Fig. 7). The southern end of this horst almost crops out. On the ES14 profile, the transitional domain is characterized by a basement high in the centre of a wide (15 km) and thick (1250 m) basin of syn-OCT and post-rift sediments. Magnetic anomalies observed in the oceanward OCT are, as on the ES12, not identified as typical oceanic magnetic anomalies related to magnetic timescale

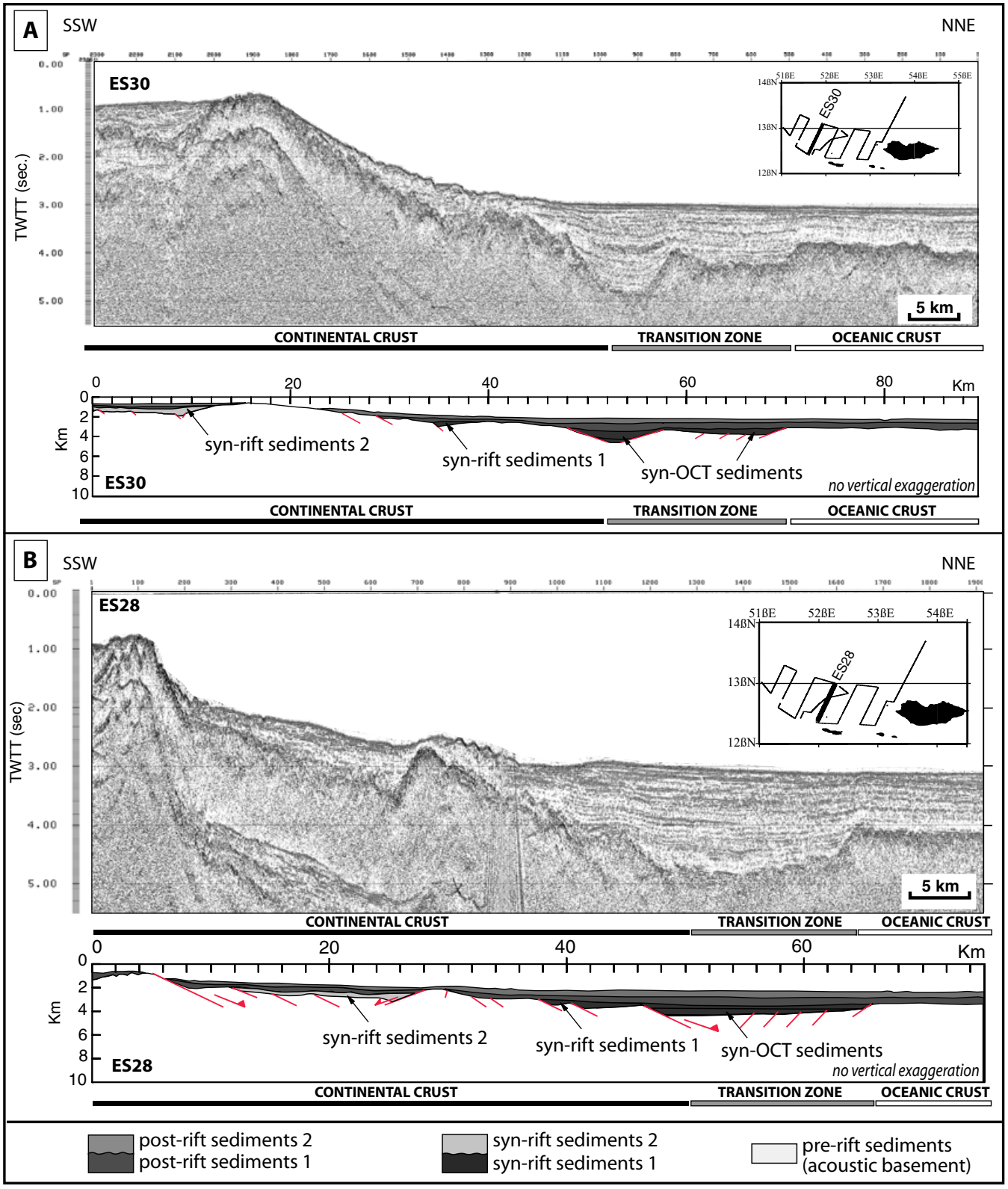

Figure 6. (A) ES30 profile of the western part of the south margin. Migrated seismic line and its interpretation. (B) ES28 profile of the central part of the southern margin. Migrated seismic line and its interpretation.

(d'Acremont *et al.* submitted). Even if syn-OCT sediments are confined to the slope foot basin, the basement horsts are included in the OCT according to the negative gravity gradient of the free-air anomaly.

The OCT boundaries are difficult to localize on some profiles. Westward, close to the Alula-Fartak fracture zone, the OCT shows a basement horst at the toe of the slope, which bounds a highly fractured deeper basement (ES06 profile, Fig. 7a). On ES12, beyond

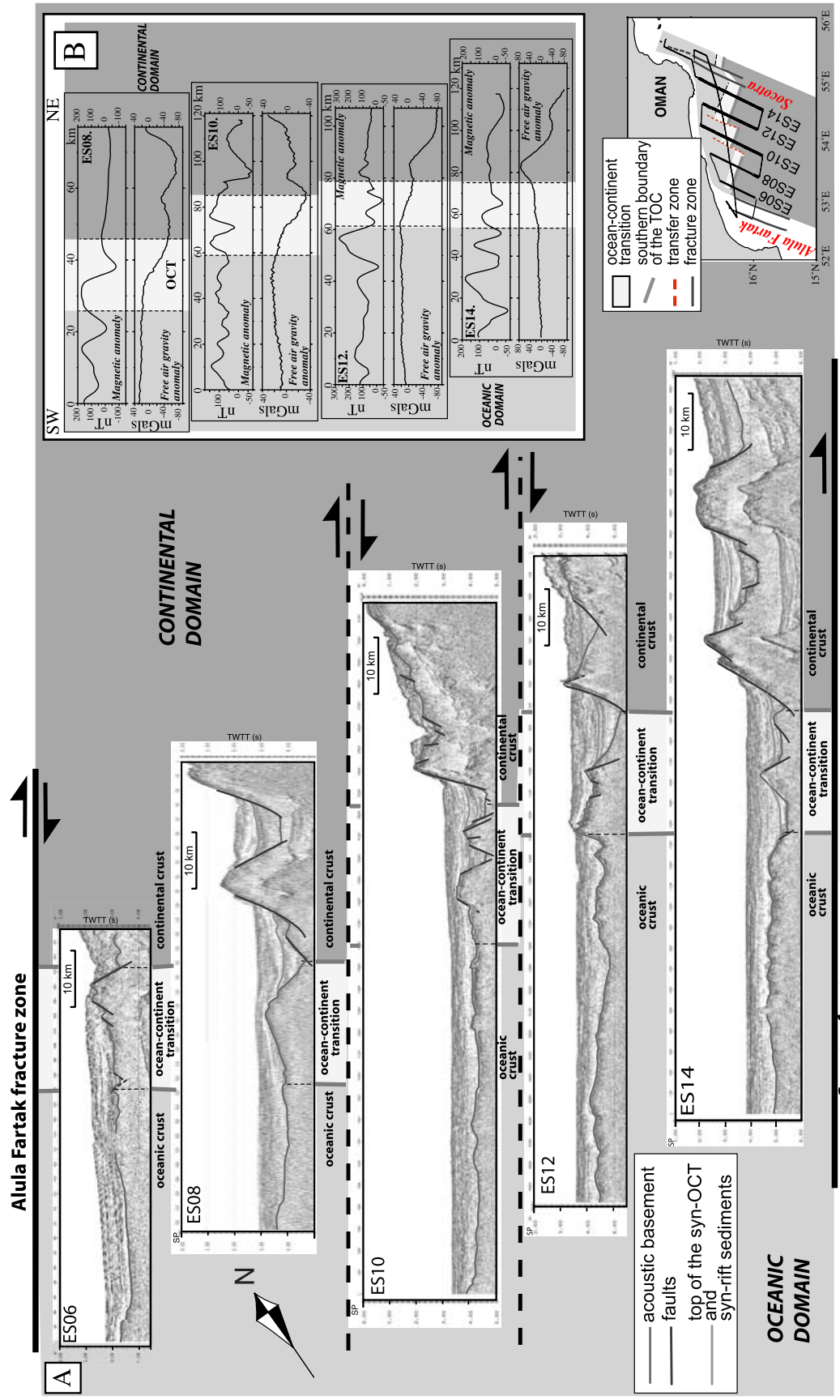

Figure 7. (A) Sketch of the evolution of the northern OCT from the Alula-Fartak fracture zone to the west to the Socotra fracture zone to the east. See inset map for the location. The map (inset) shows the location of the different structures described on the profiles and on the background map. See text for description of profiles and interpretation. (B) Gravity and magnetic profiles over the OCT from west (top) to east (bottom).

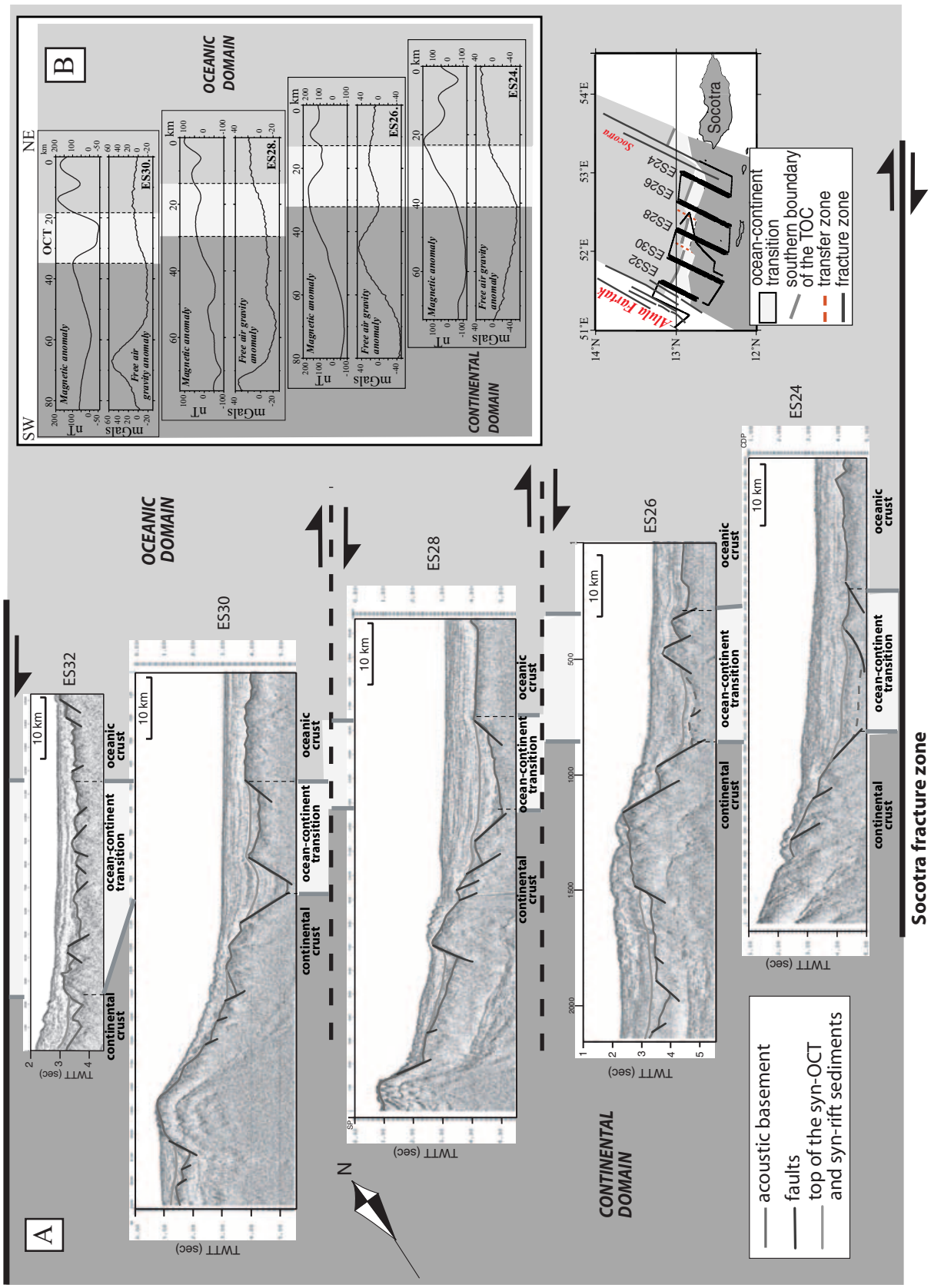

Figure 8. (A) Sketch of the evolution of the southern margin OCT from the Alula-Fartak fracture zone in the west to the Socotra fracture zone in the east. See inset map for the location. The map (inset) shows the location of the different structures described on the profiles and on the background map. See text for description of profiles and interpretation. (B) Gravity and magnetic profiles over the OCT from west (top) to east (bottom).

the northern OCT boundary, the magnetic and gravity signals seem to correlate with the edge effect of the last continental tilted block (Figs 7a–b). On the ES14 profile, only the magnetic and seismic reflection data help to identify the northern boundary of the OCT. Indeed, the free-air gravity anomaly is characterized by a positive gradient toward the continental domain (Fig. 7b). The magnetic signal is flat northwards of the deepest continental basement high which is underlined by a free-air anomaly high, followed by a sudden drop, from +75 to −40 mGal.

Southern margin OCT. On the southern margin, the OCT is characterized by a wide rifted basin at the foot of the continental slope (Fig. 8). This basin is asymmetric, with major northward-dipping faults and several antithetic and close (2–3 km) southward-dipping normal faults (Fig. 8). The width of the basin varies from 10 to 20 km, depending on which antithetic faults preferentially developed. On the ES26 profile, the free-air anomaly is positive over the two basement ridges which bound the southern flank of the basin. Westward, close to the Alula-Fartak fracture zone, the OCT is broad and faulted (ES32 profile, Fig. 8). The southern OCT does not display magnetic anomalies (Fig. 8).

The filling of the slope foot basin reaches 2 km on profile ES30, including a 500–900 m thick layer of syn-OCT sediments (Fig. 7). A comparable basin is imaged eastwards, close to the Socotra fracture zone (ES24; Fig. 8a).

The ES28 profile shows that syn-OCT series extend southwards on the deep northern-tilted block of the margin, where they form a fan-shaped wedge (Figs 6 and 8a). Accordingly, the syn-OCT sediments correlate with upper syn-rift series.

4.2.3 Oceanic domain

The oceanic domain is characterized by a gentle basement topography with isolated volcanic seamounts (Fig. 2, northeast flank of the basin; 16.2°N 54.8°E) and a lack of faulted sediments. The top of the basement is 1 km shallower than in the OCT along both margins. The acoustic basement shows a more regular topography than the continental and OCT domains (Figs 7 and 8). It presents a highly reflective uppermost layer due to the chaotic pattern of the crust, contrasting with the smooth seismic signal of the continental crust. The two post-rift sequences recognized in the continental domains cover both flanks of the basin with a 1.5 km maximum thickness. The crust displays oceanic magnetic anomalies that can be correlated with the magnetic reversal timescale (d'Acremont *et al.* submitted).

5 SEGMENTATION AND STYLE OF DEFORMATION ON CONJUGATE MARGINS

The Alula-Fartak and Socotra fracture zones express the first-order segmentation of the study area (see Figs 1 and 10). A second-order segmentation is evidenced by the Encens–Sheba data between the Alula-Fartak and Socotra fracture zones. On the northern margin, northeastward *en echelon* offsets of the structures (normal faults, basins, horsts, OCT) reveal three segments separated by N30°E-trending transfer zones (Figs 9 and 10). These two 25 km offset transfer zones are imaged on the seismic lines parallel to the margin as negative flower structures, which suggest the existence of accommodation zones (Fig. 9). The offsets are less important on the southern margin, the central segment being shifted by 9 km and 12 km with respect to the western and eastern segments respectively. On both margins, the central segment is shorter than the two adjacent ones (Table 1).

6 OFFSHORE–ONSHORE LINKS

6.1 Northern offshore–onshore links

The emerged continental zone affected by the Oligo-Miocene rifting spans over more than 100 km along the NNE–SSW opening direction, in the Dhofar region, the Ashawq-Salalah Plain and the Haluf, Sala'Afan and Hasik grabens (Figs 1, 2 and 10). The difference in investigation methods makes it difficult to correlate the offshore and onshore structures. However, in the Dhofar area, although normal faults dip either toward the continent or the ocean, most are seaward-dipping faults. South of the Ashawq graben, several N110° E normal structures can tentatively correlate with normal faults identified on the offshore seismic profiles (Fig. 10). No N30°E strike-slip faults were recognized onshore (Lepvrier *et al.* 2002). On the western edge of the major Ashawq Basin, the N45°E to N70°E normal faults occurring in the onshore continuation of the Alula-Fartak fracture zone do not present any strike-slip component, and are interpreted as faults generated by a local stress perturbation due to oblique slip on the major border fault of the Ashawq Basin (Bellahsen *et al.* in press). The lack of strike-slip faults onshore is not consistent with the *en echelon* basins observed offshore (Figs 9 and 10), and suggests a diachroneity in development of early syn-rift and late syn-rift segmentation. This could be due to different mechanical responses to the extensional stress field of the thinned continental lithosphere, close to the palaeorift, and farther, on the upper part of the margin.

6.2 Southern offshore–onshore links

Socotra Island and eastern Somalia display extensional features, which represent the continental emerged margin (Figs 1 and 10). Close to the Indian Ocean, the Jurassic and Cretaceous extension strongly structured the continental lithosphere prior to the Oligo-Miocene rifting. On the eastern edge, the northern Somalia Basin was formed in Late Jurassic and Early Cretaceous, in response to the southward movement of East Gondwanaland (Madagascar and India) relative to Africa–Somalia (Cochran 1993). The N45°E-trending faults related to this extension are dominant in the southeast Socotran Platform (Birse *et al.* 1997). A correlation between the Oligo-Miocene extensional features onshore and offshore is possible in the western part of Socotra Island, where the N110°E onshore normal faults continue offshore. In eastern Somalia, the continental emerged zone involved in the Oligo-Miocene rifting reaches a width of 150 km, including the Alula, Quandala and Bosaso-Darror basins, where the major normal faults dip toward the continent (Fig. 1, El Gal and Darror faults) (Fantozzi & Sgavetti 1998).

7 DISCUSSION

7.1 Non-volcanic passive margins

The Gulf of Aden is one of the three rifts that join at the Afar hotspot, and whose Oligocene opening is synchronous with initial flood basaltic magmatism at ∼31 Ma. Studies in the western part of the Gulf highlight the influence of the Afar hotspot on the structure of the oceanic basin and its conjugate margins (Tard *et al.* 1991; Hébert *et al.* 2001). Off Aden city (Fig. 1), the foot of the northern continental margin is characterized in the seismic data by the presence of seaward-dipping reflectors (Tard *et al.* 1991). These volcanic wedges, whose thickness ranges from 150 m onshore to 6 km offshore, are Oligo-Miocene in age. No data are available on

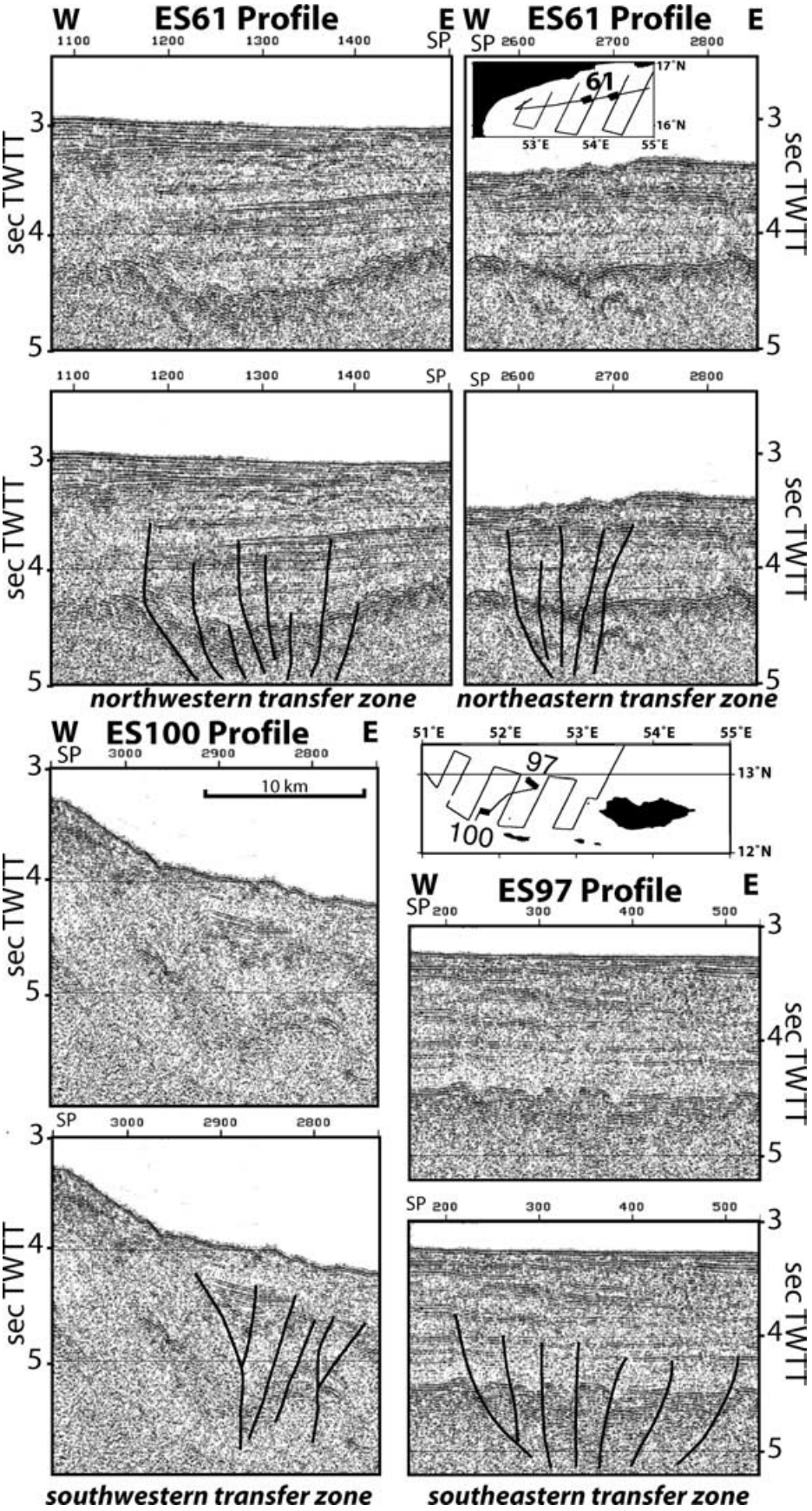

Figure 9. Seismic profiles crossing the accommodation zones in the northern and southern margins and showing the associated negative flower structures.

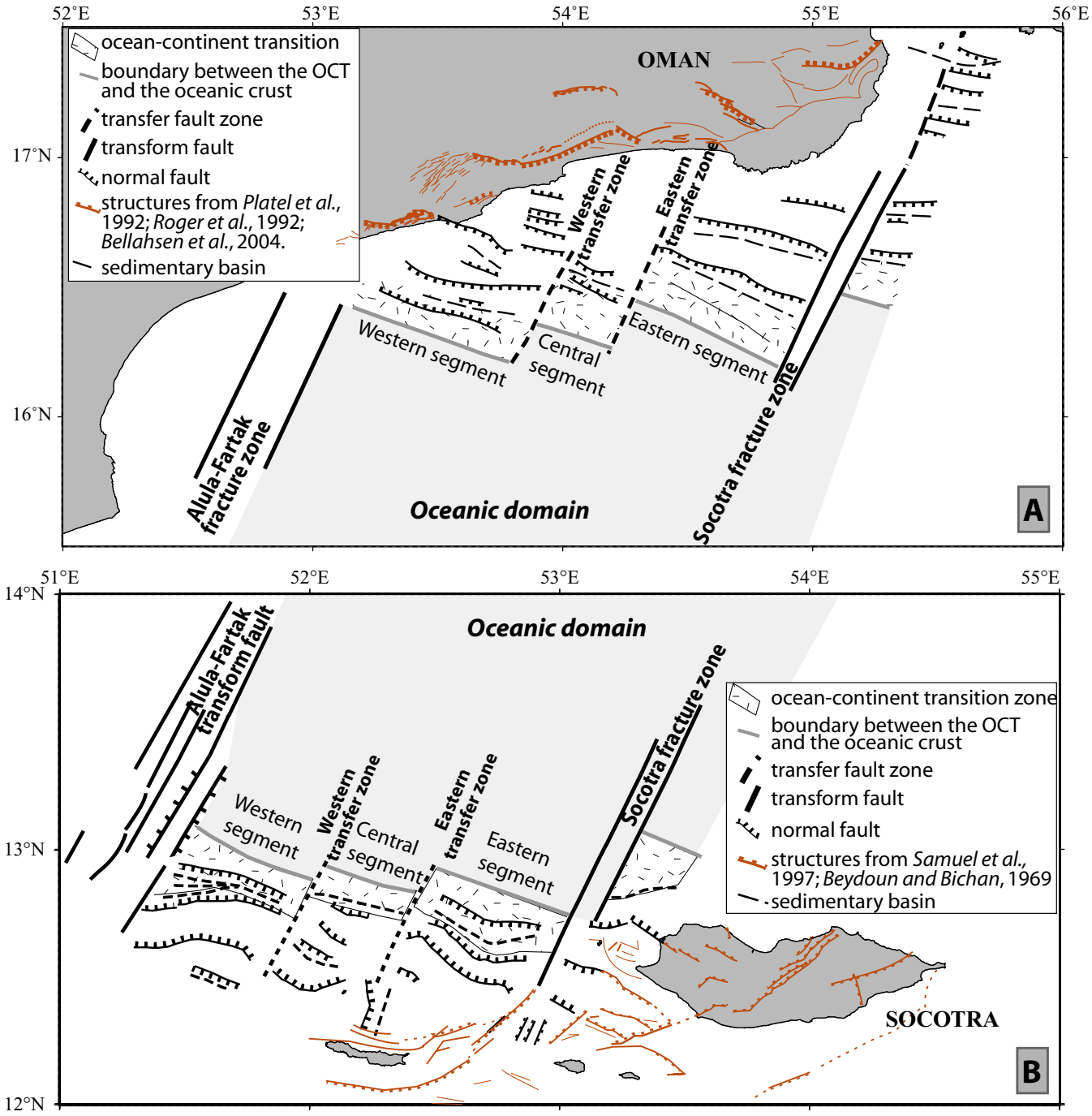

Figure 10. Interpreted structural map of the whole northern and southern margins.

the southern margin. Although the northern margin is described as volcanic up to 44.7°E and volcanic material exists in the east of the Shukra-El Sheik discontinuity (Tard *et al.* 1991), this morphostructural discontinuity is considered as the eastern limit of the influence of the Afar hotspot (Hébert *et al.* 2001, and references therein).

Located at about 850 km east of the Afar hotspot, the study area does not show any evidence of syn-rift volcanism, suggesting that the surface expression of the plume did not extend past the Alula-Fartak fracture zone region. Neither SDRs nor flat and highly reflective volcanic flows are imaged in the OCT or on the margins by our seismic data. This is in agreement with the onland stratigraphy of the upper margins, which does not include syn-rift volcanic series. This general lack of volcanic series in the syn- and post-rift succession of northeastern Somalia and southern Oman shows that the mechanism of continental lithosphere breakup in the eastern Gulf is not directly influenced by the Afar hotspot.

7.2 Ocean–continent transition

Our data evidence a transitional domain of uncertain affinity between the fault blocks of thinned continental crust and a domain that displays geophysical characteristics of oceanic crust.

The nature and evolution of the OCT, in non- or weakly volcanic margins, is still poorly constrained, partly because of the scarcity

Table 1. Synthesis table of the main structural features of the conjugate margins and comparison: W, western segment; C, central segment; E, eastern segment.

	North margin	South margin	Total (north + south) or difference (Δ = north − south)
Segment length (E–W)	W: 77 km C: 33 km E: 70 km	W: 60 km C: 42 km E: 60 km	W: $\Delta = +17$ km C: $\Delta = -9$ km E: $\Delta = +10$ km
Margin width (N–S) including the totality of the rifted zone (Fig. 12)	W: 125 km C: 125 km E: 140 km	W: 300 km C: 300 km E: 300 km	W: 425 km C: 425 km E: 440 km
OCT width	W: 20 km C: 26 km E: 21 km	W: 16 km C: 16 km E: 19 km	W: 36 km C: 42 km E: 40 km
Segment shift at the OCT–oceanic crust boundary	W–C: 19 km C–E: 23 km	W–C: 9 km C–E: 14 km	W–C: $\Delta = +10$ km C–E: $\Delta = +9$ km
Depth of the acoustic basement (at the OCT–oceanic crust boundary)	W: 2.7 km C: 3.2 km E: 2.7–4.3 km	W: 3.2 km C: 3.3 km E: 3.1–3.8 km	W: $\Delta = -0.5$ km C: $\Delta = -0.1$ km E: $\Delta = -0.4, +0.5$ km
Mean thickness of the post-rift sediments (at the OCT–oceanic crust boundary) (m below sea level)	W: 600 m C: 800 m E:100–1300 m	W: 1100 m C: 1000 m E: 600–1400 m	W: $\Delta = -500$ m C: $\Delta = -200$ m E: $\Delta = -100, -500$ m
Mean thickness of the syn-rift sediments	W: 1000 m C: 600 m E: 650 m	W: 1200 m C: 750 m E: 900 m	W: $\Delta = -200$ m C: $\Delta = -150$ m E: $\Delta = -250$ m

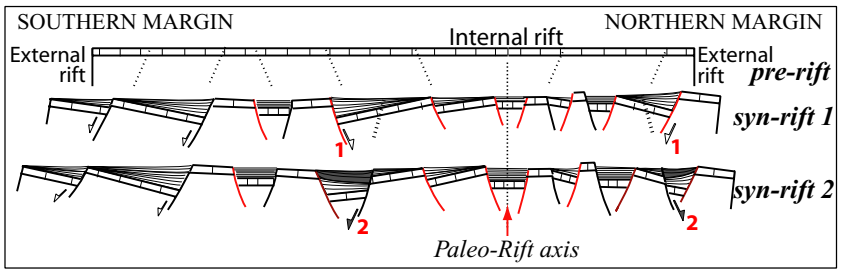

Figure 11. Interpretative sketch of the margin structure, which shows the two observed syn-rift sequences and the re-partition of the vergence of the faults in relation to the two syn-rift episodes. Note the deformation wavelength and width asymmetries between both margin.

of well-studied examples. On the western Iberian margin, the basement in the OCT, which is structured in 20–25 km wide horsts and grabens, is mainly made of serpentinized peridotite over a width varying from 30 to 130 km (Boillot *et al.* 1988; Beslier *et al.* 1996; Whitmarsh *et al.* 2001). These mantle rocks were exhumed under the rift zone and tectonically denuded at the palaeorift axis at the end of the breakup. Serpentinization is due to water circulation during the late stages of mantle exhumation. The thin (4–5 km) seismic crust corresponds to the serpentinized uppermost mantle, which is buried under the sedimentary cover. The intense deformation of the mantle rocks and the scarcity of partial melt products show that tectonics prevails over magmatism during the formation of the OCT. It suggests that the exhumed mantle was stretched on the seafloor until the onset of true oceanic accretion. This possible scenario would have some analogies with ultraslow spreading ridges, which create a heterogeneous oceanic seafloor made of serpentinized mantle and associated partial melt products in variable proportions (Cannat 1993). Northward on the Galicia margin, the OCT is narrower (±30 km) and composed of a single horst of exhumed mantle rocks bounded by two deep basins (Boillot *et al.* 1988). OCTs made of exhumed mantle also exist in the Tyrrhenian and Red seas and along the southwest Australian margin (Nicolas *et al.* 1987; Bonatti *et al.* 1990; Beslier *et al.* 2004). This tends to generalize the existence of exhumed mantle OCTs in non- or poorly volcanic extensional systems, and the idea that oceanic spreading may not succeed immediately to continental breakup. However, the hypothesis of an OCT made of thinned continental crust cannot be excluded, provided that the width of this OCT does not exceed a few tens of kilometres, beyond which ongoing thinning leads to the breakup of the mechanically weak continental crust.

In our study area, no samples and only indirect data are available which do not allow us to determine the nature of the basement in the OCT, but we can hypothesize using these other margins as analogues. We present here a few clues gathered from our data.

The total width of the OCT, margin to margin, averages 40 km (Table 1, Fig. 10). Gravity highlights a crust thinned to about 4 km (Leroy *et al.* 2004). The structure of the basement in basins and horsts shows that tectonics prevailed over magmatism during the formation of the OCT. Faulted sediments are observed between the acoustic basement and the post-rift series on the whole south OCT and in the slope foot basin of the north OCT. These syn-OCT series are thus older than post-rift series. One seismic line on the south margin (ES28) shows the correlation between upper syn-OCT and upper syn-rift series on the deep margin. Accordingly, the

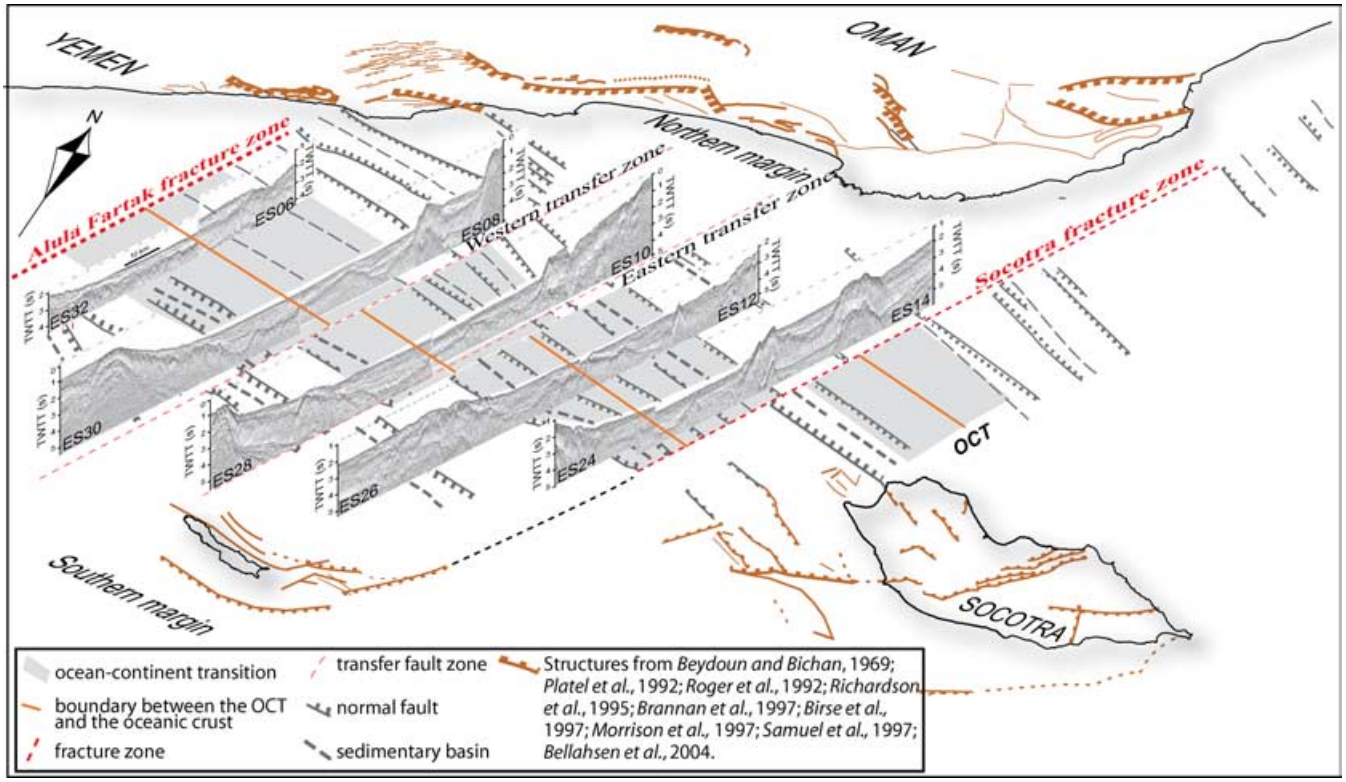

Figure 12. Comparison of the conjugate margins without the oceanic crust. Sketch of the Encens–Sheba profiles joined at the same depth (TWTT sec) at the boundary between the OCT and oceanic crust.

basement in the OCT basins should be made of thin continental crust intruded or not by magmatic bodies. This hypothesis is in agreement with the general lack of magnetic anomalies in these areas (Figs 7b and 8b).

A different nature for the basement may be suspected in the southern half of the north OCT where magnetic anomalies are recorded. There, the faulted basement displays one or two 10–15 km wide horsts buried under post-rift sediments. The absence or scarcity of syn-OCT sediments may be due to the deep slope foot basin acting as a trap for the sediments coming from the nearby continental margin. These features clearly contrast with the relatively flat basement of the adjacent oceanic domain. The characteristics of this part of the OCT are consistent with two possible origins: either an exhumed mantle or an ultra-thinned continental crust, possibly intruded by partial melt products of the underlying mantle in variable proportion. Further geological and geophysical investigations are needed to choose between these two hypotheses. According to the first hypothesis, the north margin would be comparable to the Galician margin: a narrow OCT made of exhumed and faulted mantle, and a deep slope foot basin where the boundary with the thin continental crust of the margin occurs.

In conclusion, a large part of the OCT may be made of very thin continental crust and the OCT is the result of the progressive localization, during the rifting and ongoing extension, of the deformation and thinning of the continental crust at the rift axis. At one point, the continental crust finally broke off and two hypotheses are proposed depending on the nature of the basement in the southern half of the north OCT:

(1) either the oceanic spreading proceeds after the intrusion in the very thin continental crust of the deep north margin of some partial melt products of the underlying mantle, or

(2) by analogy with older passive margins, the oceanic accretion is delayed or ultraslow, and the mantle is exhumed in the continental crust breakup zone and then stretched over a few kilometres before the beginning of true oceanic crust accretion.

The true oceanic spreading then takes place between a thin continental crust (southern OCT) and a heterogeneous crust (southern part of the northern OCT), suggesting an asymmetric tectonic process.

7.3 Tectono-sedimentary evolution of the conjugate margins

7.3.1 Syn-rift event (from upper Eocene to middle Miocene; 35–18 Ma)

In the offshore basins of the 'Encens–Sheba' area, the syn-rift sediments are less than 1200 m thick. This thin syn-rift sequence is consistent with the 1400 m thickness of the syn-rift series in the Dhofar area (Roger *et al.* 1989). The margins are mainly structured by conjugate faults, which create slope deposits which may or may not be followed by horizontal series. The syn-rift series generally do not show fan-shaped geometries indicative of syn-depositional faulting. However, several fan-shaped geometries are identified in the basin on both margins, with a peculiar pattern of two superimposed fans with opposite polarities. The opposite fan geometries are generated by the successive movement of the antithetic dipping border faults of the basin, the first one occurring along the oceanward-dipping fault. These two syn-rift phases could be associated with successive uplifts of the rift shoulders. Elsewhere, the syn-rift series, often thinner, rarely display fan-like sedimentary wedges. One

explanation may be the oblique opening of the rift. Small-scale analogue models indeed show that the fan-like sedimentary wedge obtained with perpendicular extension is almost completely absent when the extension is oblique (Tron & Brun 1991). It also seems difficult in such oblique opening models to draw from the fault pattern a simple evolution of the rift zone in term of symmetry and distribution of the deformation.

In the OCT, faulted formations are identified, in between the basement top and the base of post-rift 1 sequences. These deposits seem to be coeval with the syn-rift series. The deposition took place during the deformation of the basement in the OCT zone, in the breakup zone of the continental crust (Figs 7 and 8). As previously proposed, these series probably overlap thinned continental crust.

7.3.2 Post-rift event (middle Miocene to present; 18–0 Ma)

Post-rift sediments are almost missing on the onshore conjugate margins. The margins reach their present morphology and position at the rifting end (Roger *et al.* 1989). Offshore, from seismic interpretation results, the post-rift deposit marks one complete regressive and transgressive cycle, corresponding to uplift and subsidence episodes after the formation of the breakup unconformity.

The first half cycle (regressive) corresponds to the maximum shoulder uplift, synchronous with the end of rifting and the breakup of the continental crust. The almost total marine regression involves a strong erosion of the new relief. The shoulder tilting rejuvenates the main boundary faults of Dhofar and eastern Somalia. This new accommodation space allows the offshore accumulation of >1000 m of post-rift sediments, which, in some places, possess a fan morphology indicative of a syn-faulting deposit (post-rift 1 series). The post-rift 1 unit, unconformable on the syn-rift and syn-OCT units eroded on the top, is identified offshore by a hummocky seismic facies and continuous horizontal reflectors, maybe associated with salt deposits during drop in sea level.

The second half cycle (post-rift 2) results from the last marine incursion which is associated with thermal subsidence and the formation of the continental slope. It is characterized by slump deposits at the foot of the slope. On seismic profiles, the onlap reflector terminations indicate a transgressive phase above the post-rift 1 deposits. These sequences are poorly represented onshore, where they are composed of reef deposits and conglomeratic sandstones (Shihr 3 group, Adawnib and Nar formations: Platel & Roger 1989; Watchorn *et al.* 1998).

7.4 Margin asymmetry and inheritance

The structural study of the conjugate passive margins reveals several differences on both margins. The comparative results are reported in Table 1. The accuracy of these measurements must be balanced against the density of seismic lines.

The seismic profiles joined on the true oceanic crust boundaries (see Fig. 12) show sections of the stretched domain just before the onset of the oceanic spreading. This reconstruction allows us to compare the sediment thickness between the two margins (Table 1) and the depth of the acoustic basement at the OCT. The thicker post-rift sedimentary sequence suggests that the subsidence is more important on the southern margin (difference ranging from -0.1 to 0.5 km; Table 1). This is possibly due to more important pelagic, river deposits and/or a more important thermal subsidence associated with a hotter mantle. This last hypothesis is consistent with the presence of a thermal anomaly beneath the southern part of the basin related to the offset of the Aden Ridge along the Alula-Fartak fracture zone. Indeed, a singularity of the southern region is the location of the Aden spreading axis, west of the Alula-Fartak transform fault, at the same latitude and close to the southern margin (Fig. 2B; 4500 m deep nodal basin situated at 51°15E). Since the end of the rifting, the ridge has run northwards along the northern half of the south margin (see also Fig. 13). The thermomechanical consequences of this ridge-related thermal anomaly on the adjacent southern half of the studied area can include an increased subsidence and a post-rift sedimentation (Table 1; Fig. 11).

The basin width depends on the depth to detachment of the normal faults, as the brittle–ductile boundary or the detachment level (Allemand & Brun 1991). On the northern margin, the basin width is more important onshore ($\sim$30 km) than offshore ($\sim$15 km; Figs 11 and 12). This decreasing width towards the ocean is consistent with the higher crustal thinning towards the rift axis.

Fig. 13 is a geological and structural reconstruction of the eastern Gulf of Aden in Miocene time (20 Ma), with a fit of the conjugate margins along the oceanward boundary of the OCT, meaning that the true oceanic domain is removed. This fit shows the relationship between pre- and syn-rift tectonic features on the Socotran Platform and northeastern Somalia to the south and those observed in eastern Yemen and southern Oman to the north. Taking into account the onshore stretched domains, the south margin is about twice as large as the north one (Fig. 13 and Table 1). The north rifted continental domain is less than 180 km wide whereas the southern one is about 300 km wide taking into account the last occurrence of syn-rift sediments eastward of the Darror Fault (Figs 1 and 13).

The strong Jurassic and Cretaceous inheritance should be invoked to explain this asymmetry. The structural and sedimentary evolution of the studied area is linked to the evolution of the eastern and northern passive margin boundaries of the Somalia Plate: to the east, the continental margin of the Indian Ocean formed in the Late Cretaceous–Palaeogene in association with the northwest–southeast to east–west opening of the Mesozoic basins, and to the north the continental margin developed in the Oligo-Miocene which is related to the opening of the Gulf of Aden (Bosellini 1986).

A huge northwest–southeast basin exists on the southern margin, between the Socotran Platform and the Alula Basin (Figs 1 and 13). According to the reconstruction, this basin extends toward the Indian Ocean, the Mesozoic Jeza-Qamar Basin of Yemen. Eastward in the Indian Ocean, it is named the Gardafui Basin. These basins therefore form a unique Jeza-Qamar–Gardafui Basin (Fig. 13). The reconstruction also suggests that the Oligo-Miocene continental breakup occurred on the northern edge of this huge basin, with the subsequent incorporation of the thinned continental crust of this basin in the southern margin. Then, the width difference between the conjugate rifted margins seems to be related to structural inheritance, older rifting having affected more particularly the southern margin in this part of the Gulf of Aden. The available seismic data do not allow further discussion concerning the modality of reactivation of pre-existing tectonic features, if any, and more generally the mode of lithospheric deformation (pure/simple shears).

7.5 Oblique rifting and inheritance

The lack of strike-slip faults onshore in prolongation of the N26°E-trending Alula-Fartak fracture zone suggests that this transform fault did not exist before the end of the Oligo-Miocene rifting. Indeed, the initial fit (Fig. 13) highlights the particular location of the Alula-Fartak transform fault zone in the centre of the pre-existing

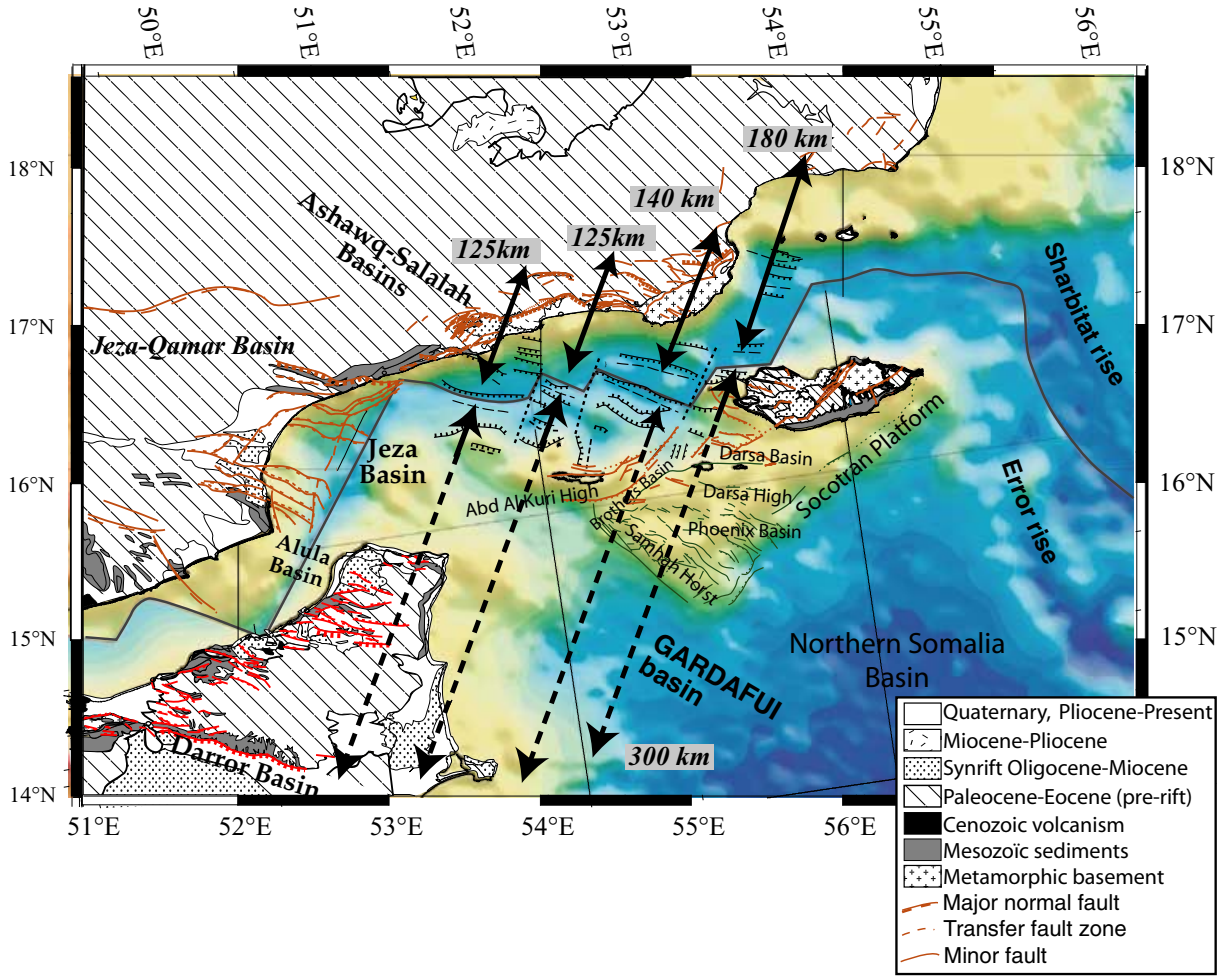

Figure 13. Miocene reconstruction of the geological and structural map of the eastern Gulf of Aden. Both margins are matched on the oceanward boundary of the OCT. Arrows show a comparison of horizontal extent of the conjugate margins.

Jeza-Qamar–Gardafui rift basin, at the rifting end. The Sheba Ridge occurs in the northern border fault of this basin, and is transformed to Aden Ridge through its southern border. The initial reconstruction is consistent with a dextral transform fault, in the centre of the Mesozoic Jeza-Qamar–Gardafui Basin, that formed during the OCT and the seafloor spreading phases (Fig. 13).

Moreover, the offshore structural map (Fig. 10) shows a normal fault network with *en echelon* basins characterized by short overlapping zones, which could be correlated to the onland structural pattern. The deformation between two adjacent basins is transferred along two transfer fault zones, which evolve as dextral transform fault zones initiated in prolongation of the transfer zones at the onset of seafloor spreading.

The northern external rift domain displays a complex fault geometry with fault directions changing from N70°E to N120°E (Fig. 10) (Lepvrier *et al.* 2002; Bellahsen *et al.* in press). On the contrary, the offshore structural pattern does not show sigmoid basins (except in the southeastern margin); faults are more systematically trending N110°E. This lack of scattered fault orientation in the offshore domain may be due to the density of seismic profiles. Fault patterns formed during oblique opening have been studied in analogue models that give asymmetrical distributions of fault direction as a function of the stretching angle (Tron & Brun 1991; McClay & White 1995; Clifton *et al.* 2000). In the case of a rift obliquity of 45°, as in the Gulf of Aden, a major fault population has a trend intermediary between the direction perpendicular to the divergence and the rift axis (here around east–west) and another fault population trends parallel to the rift axis (here N75°E). As noticed by Bellahsen *et al.* (in press), analogue models of oblique rifting do not predict more frequent N110°E-trending faults, perpendicular to the divergence. The main occurrence offshore of the N110°E fault pattern, normal to the opening direction and without scattered fault directions, could be explained with the decrease of rift obliquity influence toward the central rift.

Moreover, field data and analogue models show that reactivation is an important process during rifting in the Gulf of Aden (Bellahsen *et al.* in press). The N100–120°E normal faults on the offshore margins are subparallel to the principal extensional structures seen in the Marib–Al-Jawf–Balhaf grabens, the Masilah Basin and the eastern Jeza-Qamar Basin onshore Yemen, which are Mesozoic basins (Fig. 1). As shown by Ellis *et al.* (1996) and Huchon & Khanbari (2003), the Oligo-Miocene rifting of the Gulf of Aden reactivates these older Mesozoic basins. We assume that the Oligo-Miocene syn-rift structures along this trend are due to inherited faults, and, therefore, to a reactivation phase.

The rifting obliquity is responsible for intermediate trends between the perpendicular to the extension (N110°E) and the rift axis (N75°E), i.e. east–west, as measured in the field (Fig. 9) (Lepvrier

et al. 2002). If pre-existing faults perpendicular to the divergence are taken into account (Bellahsen *et al.* in press), the observations are consistent with the oblique rifting analogue models where the normal fault pattern is from N70°E to N120°E (Tron & Brun 1991; McClay & Dooley 1995) and with a major occurrence of N110°E-trending faults (Bellahsen *et al.* in press).

So, according to these authors we could propose that the N110°E-trending faults were formed without the dependence on rift obliquity and/or were caused by structural inheritance.

8 CONCLUSION

New single-channel seismic reflection data constrained by bathymetric, magnetic and gravity data allow us to image the shallow structure of the eastern Gulf of Aden conjugate margins and to describe contrasting tectonic styles of opening of the basin during Oligo-Miocene evolution. The Encens–Sheba data clearly demonstrate that the conjugate margins are non-volcanic in this part of the Gulf of Aden and a non- or poorly volcanic extensional regime prevailed during the continental breakup, restricting the influence of the Afar hotspot westward of the Alula-Fartak fracture zone.

Two syn-rift faulting events are identified in the offshore domain, testifying to diachronous faulting along faults dipping either towards the continent or the ocean. The base of the post-rift series indicates tectonic movement or slumping events.

Both offshore margin structures are well correlated, but several structural features show an asymmetry between the two margins. The southern margin rifted domain is about twice as large as the northern one. The crust was not homogeneous before the last Oligocene breakup as several previous rifting episodes had affected the continental Afro-Arabian crust, especially at the location of the actual southern margin of the Gulf of Aden. The offset of the Aden Ridge, west of the Alula-Fartak fracture zone, may be the cause of the higher subsidence and thicker post-rift deposits observed on the southern margin.

A first-order segmentation is expressed by the *en echelon* geometry of the rift, which persists up to now through the shift of the Aden and Sheba ridges. A second-order segmentation is highlighted offshore by our data along N26°E–N30°E-trending fracture and accommodation zones. The lack of transcurrent faults onland suggests a diachroneity in the development of early syn-rift and late syn-rift segmentation. Furthermore, the rift obliquity is responsible for fault orientation (east–west) intermediary between the perpendicular to the extension (N110°E) and the rift axis (N75°E) and for the fault orientation parallel to the rift axis (N75°E). However, the analogue models of oblique rifting do not foresee the N110°E-trending faults unless pre-existing faults are included in the initial model (Bellahsen *et al.* in press). We argue that tectonic inheritance has a substantial influence on the different styles of deformation on the same margin (from external rift to internal rift domains) and on the asymmetry between the conjugate margins. There is a reactivation of inherited Mesozoic basins in the rifted area especially on the southern margin and in the internal rift that could explain the asymmetry of the continental rifted margin.

At the end of the rifting, the deformation became localized at the rift axis, in the OCT, where sediments are faulted. The transition zone between the continental and the oceanic crusts consists of thin continental crust and possibly of exhumed mantle, intruded in variable proportion by partial melt products of the underlying mantle. When the continental crust ruptured, either oceanic spreading began (along the southern margin) or it was delayed or ultraslow (along the northern margin). In this latter case, mantle was exhumed in the breakup of the continental crust and then stretched over a few kilometres before the accretion of oceanic crust. This OCT is 40 km wide in the average OCT. Geophysical and geological information on deep crustal levels is needed in particular to investigate the mode of thinning of continental lithosphere and of transition from rifting to spreading.

ACKNOWLEDGMENTS

We thank the master and crew of R/V *Marion Dufresne* for conducting cruise operations. The Institut Polaire and SHOM teams ensured that a superb data set was collected in spite of monsoon weather. We would like to thank Cynthia Ebinger and the anonymous reviewers for thoughtful and constructive reviews. We wish to thank Philippe Patriat for helpful discussions throughout this work. We thank warmly Dr Hilal Al-Azri for his help and for the fruitful collaboration with the Directorate of Minerals of Sultanate of Oman. Waris Warsi is also thanked for his help. The Ecole et Observatoire de Physique du Globe de Strasbourg and University of Bretagne Occidentale provided technical support for the collection of seismic data. The GDRMarges provided financial support that made this cruise possible and, with the Institut National des Sciences de l'Univers, helped with the costs of data analysis. GDRMarges contribution no 2050. UMR 6526 contribution no 684. UMR 6538 contribution no 930.

REFERENCES

Ali-Kassim, M., 1993. I bacini Oligo-Miocenici della Somalia nord orientale; evoluzione sedimentaria e structturale, *PhD thesis*, University of Siena.

Allemand, P. & Brun, J.-P., 1991. Width of continental rifts and rheological layering of the lithosphere, *Tectonophysics,* **188,** 63–69.

Audin, L., Manighetti, I., Tapponnier, P., Métivier, F., Jacques, E. & Huchon, P., 2001. Fault propagation and climatic control of sedimentation on the Ghoubbet Rift floor: insights from the Tadjouraden cruise in the western Gulf of Aden, *Geophys. J. Int.,* **144,** 391–413.

Bellahsen, N., 2002. Croissance des failles normales et des rifts continentaux. Développement du golfe d'Aden et dynamique de la plaque Arabe, *PhD thesis*, Université Pierre et Marie Curie.

Bellahsen, N., Fournier, M., d'Acremont, E., Leroy, S. & Daniel, J.M. Fault reactivation and rift localization: the northeastern Gulf of Aden margin, *Tectonics*, in press.

Beslier, M.O., Cornen, G. & Girardeau, J., 1996. Tectono-metamorphic evolution of peridotites from the ocean/continent transition of the Iberia abyssal plain margin, in *Proceedings of the Ocean Drilling Program, Scientific Results,* Vol. 149, pp. 397–412, eds Whitmarsh, R.B., Sawyer, D.S., Klaus, A. & D.G. Massm, Ocean Drilling Program, College Station, TX.

Beslier, M.O. *et al.*, 2004. Une large transition continent-océan en pied de marge sud-ouest Australienne (campagne MARGAU/MD110), *Bull. Soc. géol. France,* **175,** 629–641.

Beydoun, Z.R. & Bichan, H.R., 1969. The geology of Socotra Island, Gulf of Aden, *Q. J. geol. Soc. Lond.,* **125,** 413–446.

Beydoun, Z.R., As-Sasuri, M.L. & Baraba, R.S., 1996. Sedimentary basins of the Republic of Yemen: their structural evolution and geological characteristics, *Rev. Inst. Franc. Pétrole,* **51,** 763–775.

Birse, A.C.R., Bott, W.F., Morrison, J. & Samuel, M.A., 1997. The Mesozoic and Early Tertiary tectonic evolution of the Socotra area, eastern Gulf of Aden, Yemen, *Mar. Petrol. Geol.,* **14,** 673–683.

Boillot, G., Girardeau, J. & Kornprobst, J., 1988. The rifting of the Galicia margin: crustal thinning and emplacement of mantle rocks on the seafloor, in *Proceedings of the Ocean Drilling Program, Scientific Results,* Vol. 103, pp. 741–756, ed E. Kapitan Mazullo, Ocean Drilling Program, College Station, TX.

Bonatti, E., Seyler, M., Channell, J., Girancleau, J. & Muscle, G., 1990. Peridotites chilled from the Tyrrhenian Sea, in Pro. ODP, Sci. Results, 37 – 47, 107, eds K.A. Kastens, J. Mascle *et al.*

Bonini, M., Souriot, T., Boccaletti, M. & Brun, J.P., 1997. Successive orthogonal and oblique extension episodes in a rift zone: laboratory experiments with application to the Ethiopian Rift, *Tectonics,* **16,** 347–362.

Bosellini, A., 1986. East Africa continental margin, *Geology,* **14,** 76–78.

Bosence, D.W.J., 1997. Mesozoic rift basins of Yemen, *Mar. Petrol. Geol.,* **14,** 611–616.

Bott, W.F., Smith, B.A., Oakes, G., Sikander, A.H. & Ibraham, A.I., 1992. The tectonic framework and regional hydrocarbon prospectivity of the Gulf of Aden, *J. Petrol. Geol.,* **15,** 211–243.

Brannan, J., Gerdes, K.D. & Newth, I.R., 1997. Tectono-stratigraphic development of the Qamar basin, eastern Yemen, *Mar. Petrol. Geol.,* **14,** 701–730.

Cannat, M., 1993. Emplacement of mantle rocks in the seafloor at mid-ocean ridges, *J. geophys. Res.,* **98,** 4163–4172.

Chian, D., Keen, C., Reid, I.D. & Louden, K.E., 1995. Evolution of nonvolcanic rifted margins: new results from the conjugate margins of the Labrador Sea, *Geology,* **23,** 589–592.

Clifton, A.E., Schlische, R.W., Withjack, M.O. & Ackermann, R.V., 2000. Influence of rift obliquity on fault-population systematics: results of experimental clay models, *J. Struct. Geol.,* **22,** 1491–1509.

Cochran, J.R., 1981. The Gulf of Aden: structure and evolution of a young ocean basin and continental margin, *J. geophys. Res.,* **86,** 263–287.

Cochran, J.R., 1993. Somali Basin, Chain Ridge, and the origin of the northern Somali Basin gravity and geoid low, *J. geophys. Res.,* **93,** 11 985–12 008.

Courtillot, V., 1980. Opening of the Gulf of Aden and Afar by progressive tearing, *Phys. Earth planet. Inter.,* **21,** 343–350.

d'Acremont, E., Leroy, S., Maia, M., Patriat, P., Beslier, M.O., Bellahsen, N., Fournier, M. & Gente, P. Structure and evolution of the eastern Gulf of Aden: insights from magnetic and gravity data (Encens–Sheba cruise), *Geophys. J. Int.,* submitted.

Dauteuil, O., Huchon, P., Quemeneur, F. & Souriot, T., 2001. Propagation of an oblique spreading center: the western Gulf of Aden, *Tectonophysics,* **332,** 423–442.

Ebinger, C.J. & Hayward, N.J., 1996. Soft plates and hot spots: views from Afar, *J. geophys. Res.,* **101,** 21 859–21 876.

Ellis, A.C., Kerr, H.M., Cornwell, C.P. & Williams, D.O., 1996. A tectonostratigraphic framework for Yemen and its implications for hydrocarbon potential, *Petrol. Geosci.,* **2,** 29–42.

Fantozzi, P.L., 1996. Transition from continental to oceanic rifting in the Gulf of Aden: structural evidence from field mapping in Somalia and Yemen, *Tectonophysics,* **259,** 285–311.

Fantozzi, P.L. & Ali-Kassim, M., 2002. Geological mapping in northeastern Somalia (Midjiurtinia region): field evidence of the structural and paleogeographic evolution of the northern margin of the Somalian plate, *J. Afr. Earth Sci.,* **34,** 21–55.

Fantozzi, P.L. & Sgavetti, M., 1998. Tectonic and sedimentary evolution of the eastern Gulf of Aden continental margins: new structural and stratigraphic data from Somalia and Yemen, in *Sedimentation and Tectonics of Rift Basins: Red Sea–Gulf of Aden,* pp. 56–76, eds Purser, B.H. & Bosence, D.W.J., Chapman & Hall, London.

Fisher, R.L., Bunce, E.T. & the scientific team, 1974. *Initial Reports of the Deep Sea Drilling Project, sites* 231–238, Vol. 24, ed. L. Musich, Washington (U.S. Government Printing office).

Fournier, M., Patriat, P. & Leroy, S., 2001. Reappraisal of the Arabia–India–Somalia triple junction kinematics, *Earth Planet. Sci. Lett.,* **189,** 103–114.

Granath, J.W., 2001. The Nogal rift of Northern Somalia: Gulf of Aden. Reactivation of a Mesozoic rift, in *Peri-Tethys Memoir 6,* Mémoires du Muséum National d'Histoire Naturelle, Vol. 186, p. 15, eds Ziegler, P.A., Cavazza, W., Robertson, A.H.F. & Crasquin-Soleau, S., Muséum National d'Histoire Naturelle, Paris.

Hébert, H., Deplus, C., Huchon, P., Khanbari, K. & Audin, L., 2001. Lithospheric structure of a nascent spreading ridge inferred from gravity data: the western Gulf of Aden, *J. geophys. Res.,* **106,** 26 345–26 363.

Hopper, J.R., Funck, T., Tucholke, B.E., Larsen, H.C., Holbrook, W.S., Louden, K.E., Shillington, D. & Lau, H., 2004. Continental breakup and the onset of ultraslow seafloor spreading off Flemish Cap on the Newfoundland rifted margin, *Geology,* **32,** 93–96.

Huchon, P. & Khanbari, K., 2003. Syn-rift stress field history of the northern Gulf of Aden margin, Yemen, *Tectonophysics,* **364,** 147–166.

Jestin, F., Huchon, P. & Gaulier, J.M., 1994. The Somalia plate and the East African rift system: present-day kinematics, *Geophys. J. Int.,* **116,** 637–654.

Laughton, A.S. & Tramontini, C., 1969. Recent studies of the crustal structure in the Gulf of Aden, *Tectonophysics,* **8,** 359–375.

Lepvrier, C., Fournier, M., Bérard, T. & Roger, J., 2002. Cenozoic extension in coastal Dhofar (southern Oman): implications on the oblique rifting of the Gulf of Aden, *Tectonophysics,* **357,** 279–293.

Leroy, S., Gente, P., Fournier, M. & the scientific team, 2000. *Données et Résultats Préliminaires de la Campagne MD117 ENCENS-SHEBA,* IPEV Report, p. 87, Institut Polaire Français Paul-Emile Victor, Plouzané.

Leroy, S. *et al.*, 2004. From rifting to spreading in the eastern Gulf of Aden: a geophysical survey of a young oceanic basin from margin to margin, *Terra Nova,* **16,** 185–192.

Lister, G.S., Etheridge, M.A. & Symonds, P.A., 1986. Detachment faulting and the evolution of passive continental margins, *Geology,* **14,** 246–250.

Manighetti, I., Tapponnier, P., Courtillot, V., Gruszow, S. & Gillot, P.Y., 1997. Propagation of rifting along the Arabia-Somalia plate boundary: the Gulfs of Aden and Tadjoura, *J. geophys. Res.,* **102,** 2681–2710.

Manighetti, I., Tapponnier, P., Gillot, P.Y., Jacques, E., Courtillot, V., Armijo, R., Ruegg, J.C. & King, G., 1998. Propagation of rifting along the Arabia-Somalia plate boundary: into Afar, *J. geophys. Res.,* **103,** 4947–4974.

Mauffret, A., Contrucci, I. & Brunet, C., 1999. Structural evolution of the northern Tyrrhenian Sea from new seismic data, *Mar. Petrol. Geol.,* **16,** 381–407.

McClay, K. & Dooley, T., 1995. Analogue models of pull-apart basins, *Geology,* **23,** 711–714.

McClay, K.R. & White, M.J., 1995. Analogue modelling of orthogonal and oblique rifting, *Mar. Petrol. Geol.,* **12,** 137–151.

McKenzie, D.P., 1978. Some remarks on the development of sedimentary basins, *Earth planet. Sci. Lett.,* **40,** 25–32.

Menzies, M. *et al.*, 1994. Geology of the Republic of Yemen, in *The Geology and Mineral Resources of Yemen,* pp. 21–48, eds McCombe, D.A. Fernette, G.L. & Alawi, A.J. Ministry of Oil and Mineral Resources, Geological Survey and Minerals Exploration Board, Yemen Mineral Sector Project.

Menzies, M.A., Gallagher, K., Yelland, A. & Hurford, A., 1997. Volcanic and nonvolcanic rifted margins of the Red Sea and Gulf of Aden: crustal cooling and margin evolution in Yemen, *Geochim. Cosmochim. Acta,* **61,** 2511–2527.

Morrison, J., Birse, A., Samuel, M.A., Richardson, S.M., Harbury, N. & Bott, W.F., 1997. The Cretaceous sequence stratigraphy of the Socotran platform, the Republic of Yemen, *Mar. Petrol. Geol.,* **14,** 685–699.

Nicolas, A., Baudier, F., & Montigny, R. , 1987. Structure of the Zabangacl Island and early rifting of the Red Sea, *J. geophys. Res.*, **92**, 461–474.

Platel, J.P. & Roger, J., 1989. Evolution géodynamique du Dhofar (Sultanat d'Oman) pendant le Crétacé et le Tertiaire en relation avec l'ouverture du Golfe d'Aden, *Bull. Soc. géol. France,* **2,** 253–263.

Platel, J.P., Roger, J., Peters, T.J., Mercolli, I., Kramers, J.D. & Le Métour, J., 1992. *Geological Map of Salalah, Sultanate of Oman; sheet NE 40-09,* Ministry of Petroleum and Minerals, Directorate General of Minerals, Oman.

Richardson, S.M., Bolt, W.F., Smith, B.A., Hollar, W.D. & Bermingham, P.M., 1995. A new hychocambon 'Play' area offshore Socotra Island, Republic of Yemon, *J. Petrol. Geol*., **18**, 15–28.

Roger, J., Platel, J.P., Cavelier, C. & Grisac, C.B.D., 1989. Données nouvelles sur la stratigraphie et l'histoire géologique du Dhofar (Sultanat d'Oman), *Bull. Soc. géol. France,* **V,** 265–277.

Roger, J., Platel, J.P., Berthiaux, A. & Le Métour, J., 1992. *Geological Map of Hawf with Explanatory Notes; sheet NE 39-16,* Ministry of Petroleum and Minerals, Directorate General of Minerals, Oman.

Rollet, N., Déverchère, J., Beslier, M.O., Guennoc, P., Réhault, J.-P., Sosson, M. & Truffert, C., 2002. Back arc extension, tectonic inheritance, and volcanism in the Ligurian Sea, western Mediterranean, *Tectonics,* **21,** 1–23.

Sahota, G., 1990. Geophysical investigations of the Gulf of Aden continental margins: geodynamic implications for the development of the Afro-Arabian rift system, *PhD thesis*, University College, London.

Samuel, M.A., Harbury, N., Bott, R. & Thabet, A.M., 1997. Field observations from the Socotran platform: their interpretation and correlation to southern Oman, *Mar. Petrol. Geol.,* **14,** 661–673.

Sandwell, D.T. & Smith, W.H.F., 1997. Marine gravity anomaly from Geosat and ERS1 satellite altimetry, *J. geophys. Res.,* **102,** 10 039–10 054.

Schilling, J.G., 1973. Afar mantle plume; rare earth evidence, *Nature,* **242,** 2–5.

Schilling, J.G., Kingsley, R.H., Hanan, B.B. & McCully, B.L., 1992. Nd-Sr-Pb isotopic variations along the Gulf of Aden: evidence for Afar mantle plume-continental lithosphere interaction, *J. geophys. Res.,* **97,** 10 927–10 966.

Tamsett, D. & Searle, R.C., 1988. Structure and development of the Mid-ocean ridge plate boundary in the Gulf of Aden: evidence from GLORIA side scan sonar, *J. geophys. Res.,* **93,** 3157–3178.

Tamsett, D. & Searle, R., 1990. Structure of the Alula-Fartak fracture zone, Gulf of Aden, *J. geophys. Res.,* **95,** 1239–1254.

Tard, F., Masse, P., Walgenwitz, F. & Gruneisen, P., 1991. The volcanic passive margin in the vicinity of Aden, Yemen, *Bull. Cent. Rech. Explor. Prod.,* **15,** 1–9.

Thinon, I., Fidalgo-Gonzalez, L., Réhault, J.-P. & Olivet, J.-L., 2001. Déformations pyrénéennes dans le Golfe de Gascogne, *C. R. Acad. Sci. Paris,* **332,** 561–568.

Thomas, Y., Sibuet, J.C., Nouze, H. & Marsset, B., 1996. Etude détaillée de la structure d'un bloc basculé de la marge continentale de Galice (Ouest-Ibérie) à l'aide de données sismiques acquises près du fond (système Pasisar): conséquences sur la structuration de cette marge, *Bull. Soc. géol. France,* **167,** 559–569.

Tron, V. & Brun, J.-P., 1991. Experiments on oblique rifting in brittle-ductile systems, *Tectonophysics,* **188,** 71–84.

Watchorn, F., Nichols, G.J. & Bosence, D.W.J., 1998. Rift-related sedimentation and stratigraphy, southern Yemen (Gulf of Aden), in *Sedimentation and Tectonics of Rift Basins: Red Sea–Gulf of Aden,* pp. 165–192, eds Purser, B.H. & Bosence, D.W.J., Chapman & Hall, London.

Wernicke, B., 1985. Uniform-sense normal simple shear of the continental lithosphere, *Can. J. Earth Sci.,* **22,** 108–125.

Whitmarsh, R.B., Minshull, T.A., Russell, S.M., Dean, S.M., Louden, K.E. & Chian, D., 2001. The role of syn-rift magmatism in the rift-to-drift evolution of the West Iberia continental margin: geophysical observations, in *Non-Volcanic Rifting of Continental Margins: A Comparison of Evidence from Land and Sea,* Geological Society of London Special Publication 187, pp. 107–124, eds Wilson, R.C.L., Whitmarsh, R.B., Taylor, B. & Froitzheim, N., Geological Society, London.

Wolfenden, E., Ebinger, C., Yirgu, G., Deino, A. & Ayalew, D., 2004. Evolution of the northern main Ethiopian rift: birth of a triple junction, *Earth planet. Sci. Lett.,* **224,** 213–228.